Internal instability in soils: a critical review of the fundamentals and ramifications

S. M. Dassanayake[1], A. Mousa[2*], I.M.S.K. Ilankoon[3], G.J. Fowmes[4]

[1]Graduate Student, School of Engineering, Monash University Malaysia, Jalan Lagoon Selatan, Bandar Sunway, Selangor Darul Ehsan 47500, Malaysia. Email: sandun.dassanayake@monash.edu

[2]Senior Lecturer, School of Engineering, Monash University Malaysia, Jalan Lagoon Selatan, Bandar Sunway, Selangor Darul Ehsan 47500, Malaysia. Email: ahmad.mousa@monash.edu

[3]Senior Lecturer, School of Engineering, Monash University Malaysia, Jalan Lagoon Selatan, Bandar Sunway, Selangor Darul Ehsan 47500, Malaysia. Email: saman.ilankoon@monash.edu

[4]Associate Professor, School of Engineering, University of Warwick, Coventry, CV4 7AL, UK. Email: g.Fowmes@warwick.ac.uk

*Corresponding author: ahmad.mousa@monash.edu, +60 355159611

Internal instability in soils: a critical review of the fundamentals and ramifications

Abstract

Seepage induced fine particles migration that leads to a change in hydraulic conductivity of a soil matrix is referred to as internal instability. This could jeopardize the structural integrity of the soil matrix by initiating suffusion (or suffosion): a form of internal erosion. Susceptibility to suffusion has been studied mostly under extreme laboratory conditions to develop empirical design criteria, which are typically based on the particle size distribution. The physics governing the process has not been comprehensively uncovered in the classical studies due to experimental limitations. The mainstream evaluation methods often over-idealize the suffusion process, holding a probabilistic perspective for estimating constriction sizes and fines migration. Prospective studies on constitutive modelling techniques and modern computational techniques have allowed a more representative evaluation and deeper insight into the problem. Recent advancements in the sensing technologies, visualisation and tracking techniques have equally enriched the quality of the gathered data on suffusion. This paper sets out to present the long-standing knowledge on the internal instability phenomenon in soils. An attempt is made to pinpoint ambiguities and underscore research gaps. The classical empirical studies and modern visualising techniques are integrated with particle-based numerical simulations to strengthen the theoretical understanding of the phenomenon.

Keywords: hydraulic stability, suffusion, internal erosion, dam failures

1. Introduction

Seeping water continuously washing fine particles from saturated soils in earth structures, such as zoned embankments and earth dams, can induce them internal instability. As depicted in Figure 1, the migrating fines in a soil matrix, typically the finer fraction of their particle size distribution (PSD), leave larger pore openings within the load bearing (coarser) fraction of the soil [1]. This phenomenon potentially exacerbates and weakens the physical and hydraulic performance of structures, subsequently causing settlements and structural deformations [2]. Floodwater and cyclic traffic loads induce internal instability in highway embankments and railway subgrades, resulting in collapses and long-term settlement problems [3-6]. Also, some forensic studies (e.g. [7] and [8]) have reported that internal instability in soils can lead to the formation of sinkholes and piping.

Approximately 50% of the reported embankment dam failures have been primarily caused by internal erosion [9]. As such, physical and numerical modelling of internal erosion has found a growing interest in multi-disciplinary research projects on designing, assessing performance, and monitoring embankment dams, railway cut slopes and retaining walls [10-12]. Recent studies strongly recommend the necessity of modifying the existing standards for embedment materials and design standards of these geotechnical structures to make them resilient to the consequences of internal instability driven erosion [13, 14]. Additionally, some modern resilient approaches have explored the potentials of well-designed flow-through structures in mitigating localized internal erosion and drainage [15, 16].

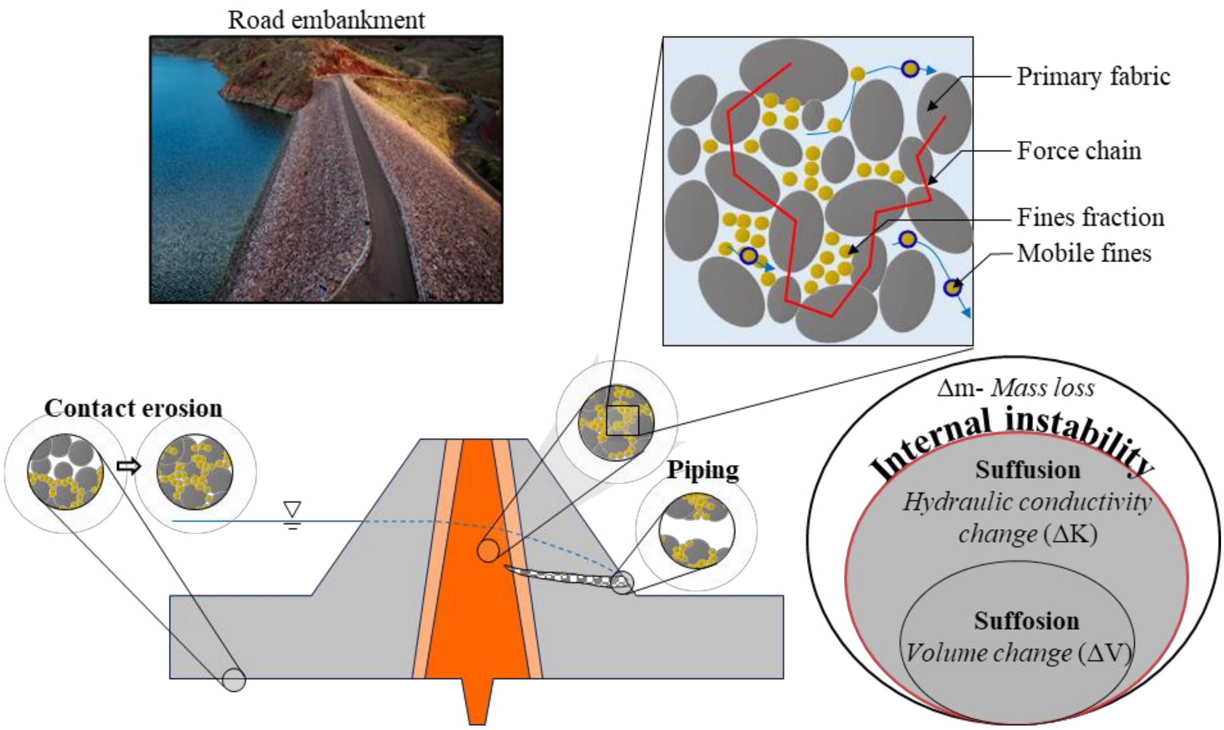

Figure 1. Internal instability and potential internal erosion mechanisms.

Internal erosion comprises four mechanisms: concentrated leak, backward erosion, contact erosion and suffusion [17]. A concentrated leak characterises a “pipe-like” eroding channel that forms in earth structures in pre-existing cracks (or hydraulic fractures), construction defects or the biological intrusions, such as animal burrows [18, 19]. In backward erosion cases, high exit gradients remove fine to medium grained soil particles (i.e., silt and sand) from the downstream surface of the earth dam creating an opening, which is also defined as piping, allowing a channel propagation to the upstream side [9]. Contact erosion occurs at the interface between coarse and fine soil layers whereby seepage parallel to the interface causes fine particles to enter the pore spaces of the coarse matrix [20]. Particularly, contact erosion causes soil losses in embankments on soft subgrades where the seeping water transports the dispersive soil particles through the larger pores of the working platform layer [21]. Suffusion occurs when the seepage flow carries fine particles in the soil matrix. When the movement of fines results in a volume change, the phenomenon is referred to as suffosion. The former should be restricted to merely describe the process associated with an observed increase (or decrease) in hydraulic conductivity. In contrast, the latter should be specifically used to describe the phenomenon only when volume change is observed [22, 23]. Moreover, the continuation of either of these processes has been shown to generate preferential flow channels that eventually lead to a concentrated leak or backward erosion, and eventually leading to all the internal erosion mechanisms [9, 12, 13].

The notion of internal instability requires a fundamental understanding in mitigating or predicting internal erosion phenomena. Again, for clarity, internal instability and fluidisation phenomena are quite distinct [26]. The latter involves the loss of effective stress in a soil mass due to the sudden increase in pore water pressure, which renders a "fluid-like" response [27] while the former relates to the process of fines migration. A contemporary technical discussion on the fluidization phenomenon in granular soils can be found in [28]. Past studies have attempted to improve the accuracy of available empirical criteria for predicting internal stability in soils and generalize them to be applicable for a wider range of different PSDs and types of soils (e.g. [29] and [30]). Available reviews on the suffusion (or suffosion), piping and backward erosion phenomena discuss the complexity and the interchangeable use of definitions related to these criteria and internal stability phenomenon in general (e.g. [9] and [23]). They collectively scrutinise internal instability in soils as an erosion mechanism but not as a soil property.

This paper reflects on the genesis and the development of internal stability assessment techniques for soils holding the perspective that this phenomenon is an inherent property associated with soil PSD. A holistic vision derived from a bibliometric analysis of the current state of the art on internal instability literature has been presented in section 2. Furthermore, the paper elaborates on conventional and empirical assessments in section 3, followed by more recent numerical and physical techniques developments in section 4. Holistically, the paper clarifies and distinguishes phenomena and mechanisms related to internal instability phenomenon for the benefit of practitioners and prospective researchers.

2. Motivation: a bibliographic insight

A bibliometric analysis was conducted using the search terms "internal instability" and "suffusion" or "suffosion" on Science Citation Index Expanded (SCI-E) in Clarivate Analytics' ISI - Web of Science© (https:// webofknowledge.com/) on August 10, 2021. The database of articles published between 2000 and 2021 yielded a search result of 246 articles. Figure 2a shows co-occurrence and the relative frequency of the search terms found in keywords, title, and the abstract of the documents. The proportional size of the nodes indicates the relative frequency of terms, whereas the thickness of the connectors indicates the frequency of their co-occurrence. Figure 2b shows the countries with the highest number of publications (at least five) and citations in this domain. Most of these countries have great number of aging geotechnical structures such as embankments, dikes, levees, and railroad systems that continuously experience cyclic loading conditions. Moreover, the studies have focused on predicting structural health and improving design guidelines for these structures.

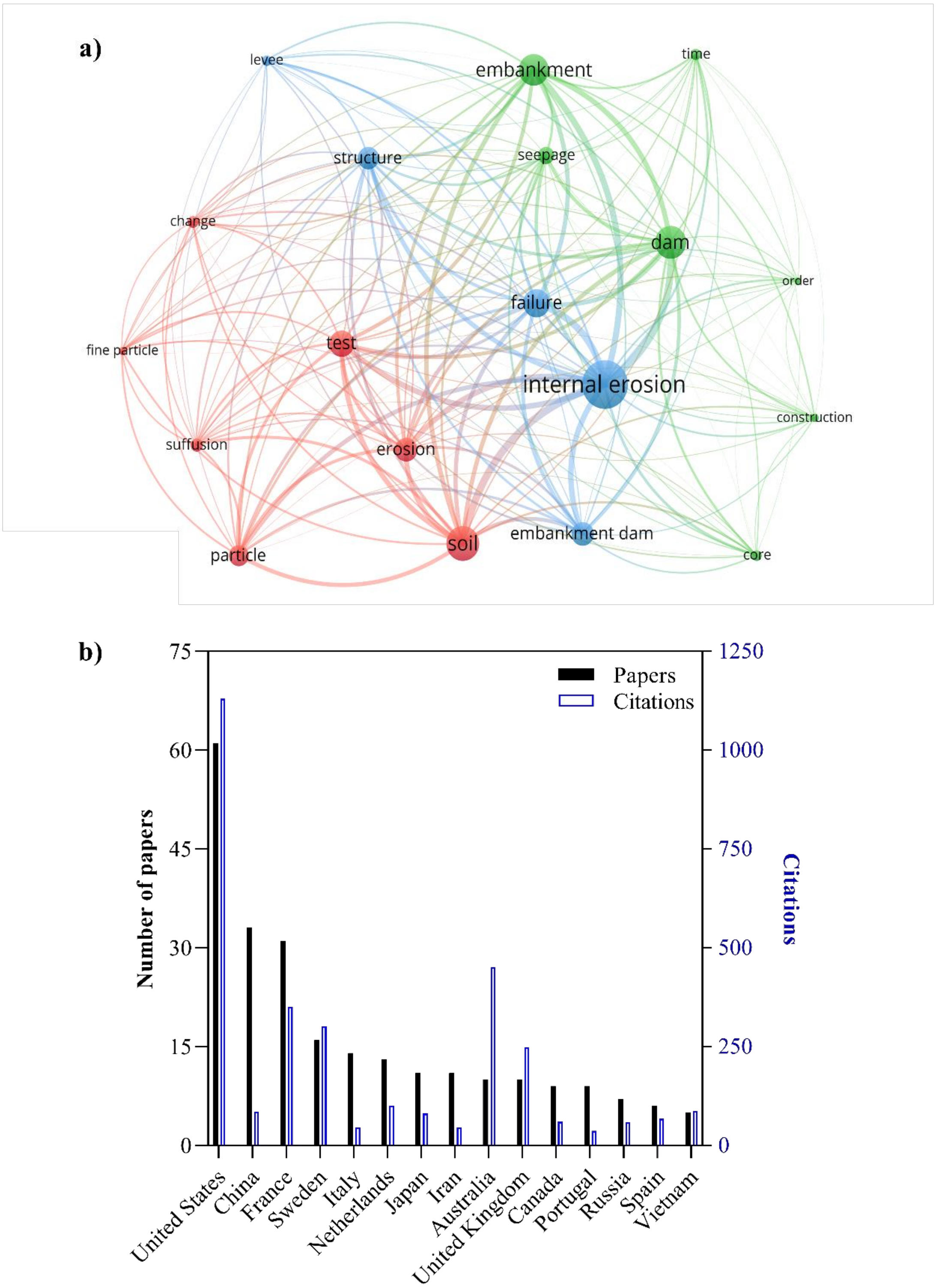

Figure 2. Publication trend from the Web of Science (WoS) online database involving the topic "Internal Erosion" and title "internal instability" or "suffusion" from 2000 to 2021: a) the terms with the highest frequencies occurred in the keywords, title or abstract of a document; b) total number of publications and the citations by country.

The research articles obtained from the bibliometric search reveal that numerical simulations have rapidly gained popularity in this research domain. These studies have been inspired by the versatility and capability of numerical simulations to investigate the physical processes spanning from the micro-level to the macro-level engineering applications. A clear indication of the micro-to-macro ramification of suffusion phenomenon can be highlighted by the connectivity of the terms such as “embankment”, “dam”, “structure” with the terms “internal erosion”, “particle”, “suffusion” and “failure”. Also, the time-dependent nature of the internal instability has been frequently studied along with experimental techniques and assessment criteria. The experimental and theoretical fronts, however, have modestly reached a stagnation level. Numerical studies have become more versatile in improving design guidelines. The titles filtered out from the bibliometric search fall into three major classes:

1. The geotechnical and scientific understanding of the fundamental mechanism of internal instability
2. Failure prediction and testing criteria to assess the internal instability
3. The adaptation of the derived knowledge in applications such as embankment design

Lack of consensus on the definitions related to the internal instability phenomenon, as a whole, has resulted in a significant ambiguity in the findings. Several authors (e.g. [23], [31]) have highlighted the need for universally accepted definitions to broaden the scope of these studies. It is the authors’ stand to define internal instability as a characteristic of the soil, while suffusion or suffosion phenomena as the physical process driven by the internal instability, following the distinction between suffusion and suffosion phenomena [23] as well as the experimental insight provided in [24] on suffosion leading to piping. Moreover, the authors believe that a concise yet focused discussion of state of the art in this domain would shed light on the evolution of technical and empirical knowledge. Also, the discussion shall establish a concise comparison between contemporary evaluation methods and their limitations while referring to the implementation of the recent advancements and future improvements in this critical domain.

3. Classical assessment of internal instability

Close relevance between the genesis of internal erosion phenomena and internal instability in soils has been a challenge to overcome in designing earth dams. Most studies (e.g. [7], [32], and [33]), therefore, attempted to propose empirical rules to assess the potential internal instability of soils. These guidelines were developed under extreme laboratory conditions with the modest knowledge of the physics of the phenomenon. Although technological limitations in observing and measuring the particle migration hindered the theoretical knowledge, analytical methods were used to stochastically model the problem at the micro level. Thus, the classical assessment techniques span from the empirical evaluation of internal instability to its analytical realisation.

3.1. Background of experimental practice

Internal instability in non-plastic soils and soils with limited plasticity index (< 7) has been experimentally investigated by utilising upwards and downward unidirectional seepage through rigid or flexible wall columns. These columns, known as modified permeameters, have diameters larger than tenfold the largest particle size to minimise the preferential flow along the wall (i.e. wall effect). Rigid wall permeameters typically have a 2:1 height to diameter ratio (e.g. [34, 35, 36]) are typically used to test non-cohesive soils, whereas flexible wall cells (modified triaxial setup) are used for moderately cohesive soils [37]. Moist tamping techniques, as given in [38], and slurry compaction, as given in [39], have been employed to minimise the fine particle segregation during the compaction of non-cohesive and cohesive soils respectively. The wall flow effect, which is higher in the contact zone for rigid wall permeameters compared to the flexible wall permeameters, has been minimised by introducing waterproof rings (e.g. [40]) between the soil specimen and the side wall to prevent the preferential seepage channels.

During the experiments involving cohesive soils, the effluent colour is commonly taken as the indication for fines migration, and it allows to determine the termination point for the experiment. A clear effluent indicates that there is no further external migration of fines (no-erosion state) (e.g. [34] and [41]). The fines fraction mobilised with the effluent is qualitatively estimated by analysing the shape of the tested soil PSD (before and after). However, in the case of downward flow tests, the screen size of the bottom plate may control the size of the particles eroded with the effluent. For instance, it has been experimentally shown that the size of the aperture should be 1.5 to 2 times larger than the size of the largest grains liable to move: a smaller aperture size creates bridging whereas a larger size fails to hold the sample [40, 41]. Hence, especially for the downward flow tests, other quantitative measures, such as the specimen deformation and the PSD of the dry mass collected from the effluent have been employed to determine the no-erosion state (e.g. [37, 41, 42, 43]).

Unidirectional flow tests, mostly under downward flow, typically employ three experimental conditions: constant gradient, multi-staged gradient, and flowrate-controlled. The first involves applying a constant hydraulic gradient across the specimen until the effluent reaches a no-erosion state. As shown in Table 1, constant gradient tests usually employ extreme gradients of the or- der of 10 or above to achieve the no-erosion state in a reasonable timeframe [37, 30, 44]. Most of the empirical design guidelines have been proposed using constant high hydraulic gradients applied across the sample in the direction of the gravity. When such gradients are used the initiation point of instability cannot be identified. The second utilises stepwise constant hydraulic gradients applied over desired time intervals to simulate a hydraulic loading pattern over the total testing time. The duration of these discrete intervals has been empirically chosen based on the observations of the no-erosion state for different soil types (e.g. [45, 46, 41, 35]). They are typically around 20 minutes but rarely as high as 24 hours. Maintaining a uniform hydraulic gradient across the sample is challenging since particle clogging (or de-clogging) decreases (or increases) the local hydraulic conductivities of the specimen. The third experimental condition involves controlling the flowrate across the soil sample throughout the duration of the experiment (e.g. [47, 48, 49]). Flowrate-controlled tests allow measuring the local hydraulic gradient changes of the sample. However, controlling the flowrates in the experiments require special equipment, such as automated variable drive pumps that can adjust the applied hydraulic head while maintaining a constant flow [47].

Table 1 summarises several studies that have reported key experimental parameters, such as hydraulic gradient and the flow direction when it is other than the direction of the gravity (i.e. downward). Such information has not been explicitly reported in a majority of empirical studies. The mainstream of listed studies employed a downward hydraulic gradient and a downward flow. Some early studies have applied mechanical vibration to the soil specimen to rapidly reach the no-erosion state. However, vibration may create preferential migration channels [35] and disrupt the bridging of mobile fines on pore openings (i.e. unclogging) [50]. Clogging, which has been mentioned in the literature as self-filtration [51] could be a reason for internal stability. Thus, mechanical vibrations can reduce the self-filtration capacity of the soil, giving the soil a pseudo-instability or giving highly conservative termination points to the experiments. Therefore, the application of the mechanical vibration in these experiments has become an obsolete practice.

Internal instability could be experimentally observed if the soil sample satisfies four conditions:

1. The coarser fraction of the PSD should form a specific structure known as the primary fabric. This fraction is stationary (non-migrating) and capable of transferring imposed stresses.
2. The finer soil grains fill the void space formed by the primary fabric without transferring stresses, and they remain as moveable particles [30].
3. The diameter of the finer soil particles must be smaller than the pore throats that connect adjacent pores of the primary fabric. For instance, the pore space between four identical spherical particles with a diameter D whose centres coincide on the corners of a pyramid can accommodate a sphere of diameter 0.33D. The surfaces of this hypothetical pyramid form

four windows (i.e. constrictions) that allow the passage of spheres smaller than diameter 0.16D (refer Equation 1).

4. The seepage flow should be strong enough to detach and carry along the loose particles from the fine fraction of the soil through the constriction network of the primary fabric.

The internal instability of a soil matrix is governed by three criteria: geometric, stress, and hydraulic [1]. The first criterion describes the geometrical possibility of fines to migrate through the soil skeleton. There should be a sufficient number of constrictions larger than the size of the fines. This could be empirically estimated using the PSD of the soil. The second criterion (i.e., stress) implies that the stress applied on the soil should be small enough such that the fines can escape from the soil matrix. The third criterion (i.e., hydraulic) indicates that the momentum of the seeping water should be sufficiently large to drive mobile fines to flow through the constrictions. The stress and hydraulic criteria are fundamentally interrelated. Larger stress will hold the fines trapped in the pore space, and thus, a higher hydraulic gradient (or a push) will be needed to mobilise the fines.

Complexity in the underlying mechanisms of internal instability hinders the possibility of standardising the experimental conditions. Besides, the hydraulic and mechanical parameters controlling internal instability could not be simultaneously measured in real time until recently. Therefore, using geometric-based methods have been the mainstream approach for assessment of internal instability since they only require the PSD of the soil specimen.

Table 1 The experimental conditions of some selected internal stability assessment studies with the direction of hydraulic flow (modified after [42]).

PSD	Hydraulic gradient	Duration (h)	Source
Well graded	0.5-16	-	[52]#
	-	30–100	[34]#
	≤ 21.6	1.5	[53]#
	≤ 2.5	-	[54]
	≤ 9.8	10	[55]#
	21.0-49.0	72	[56]
	0.1-18.5	9	[35]#
Well & Gap graded	≤ 0.7 (horizontal)	0.5	[57]
	2.5-6.7*	2.5	[58]#
	≤ 20.0 (up)	-	[59]
	≤ 1.0 (up)	1.5	[60]
	0.08-31.0* (up & down)	2–5	[61]
	8.0 (up & down)	3	[30]
	0.2-0.9 (up)	500–1600	[62]
	10.0-11.0	12–612	[63]
Gap-graded	9.8-13.0	2	[51]#
	0-62 (up & down)	6–28	[39]
	5-140	0.25	[37]
	0.1-8	8	[41]
	0.6-3	0.4	[64]
	0.1-1	-	[65]
	3-5.5	0.6	[66]

*some samples were made from glass balls; #vibration applied

3.2. Geometric based assessment criteria

Geometrical criteria have been developed as empirical measures of a soil's susceptibility to internal instability. They were typically developed for well-graded non-plastic (plastic fines $<$ 5%) granular soils. Only a few criteria can be applied with confidence to cohesive soils. Soils with higher fines content (typically greater than 50 %), well-graded soils with an upwardly concave-shaped PSD or gap-graded soils are often internally unstable. Uniformly-graded soils exhibit higher stability compared to those. The classical methods (e.g. [34], [67] and [68]) used key determining particle size ratios taken from the soil PSDs as empirical measures of instability. These size-based criteria were then replaced by various mass-fraction based criteria, which employ the shape of the PSD.

Various researchers, irrespective of the extremity of the experimental conditions (as highlighted in [41]), conceptually agree on the existence of a load bearing primary fabric and a loose fines fraction in internally unstable soils. This notion supports the idea of separating the PSD into two sections (Figure 3a). The primary fabric is assumed to act as a filter for the fines fraction to maintain internal stability. Therefore, it should be coarse enough to allow flow, yet fine enough to minimise the mobilisation of the fines and achieve internal stability. Kezdi [68] proposed that a sharp transition (an inconsistency) found in the shape of PSDs of well or gap-graded soils could be hypothesised as a point that distinguishes the primary fabric from the fines fraction. The classical Terzaghi filtration criterion [69] suggests that $d_{(P,15)}$ of the primary fabric should be smaller than four times $d_{(F,85)}$ of the fines fraction [68]. Based on experimental observations, [67] (as cited in [70]) defined I_r as a ratio between the key determining particle sizes (i.e., $\frac{d_{\mathrm{P},15}}{d_{\mathrm{F},85}}$) to estimate the degree of instability. I_r values smaller than 5 indicate an internally stable soil. However, both [67] and [68] methods, which are merely based on size-ratios, have no consensus on the determining sizes that separate the PSD as primary fabric and fines fraction (Table 2). The mass fraction belonging to mobile fines cannot be predicted using these two methods without a series of trial experimental tests.

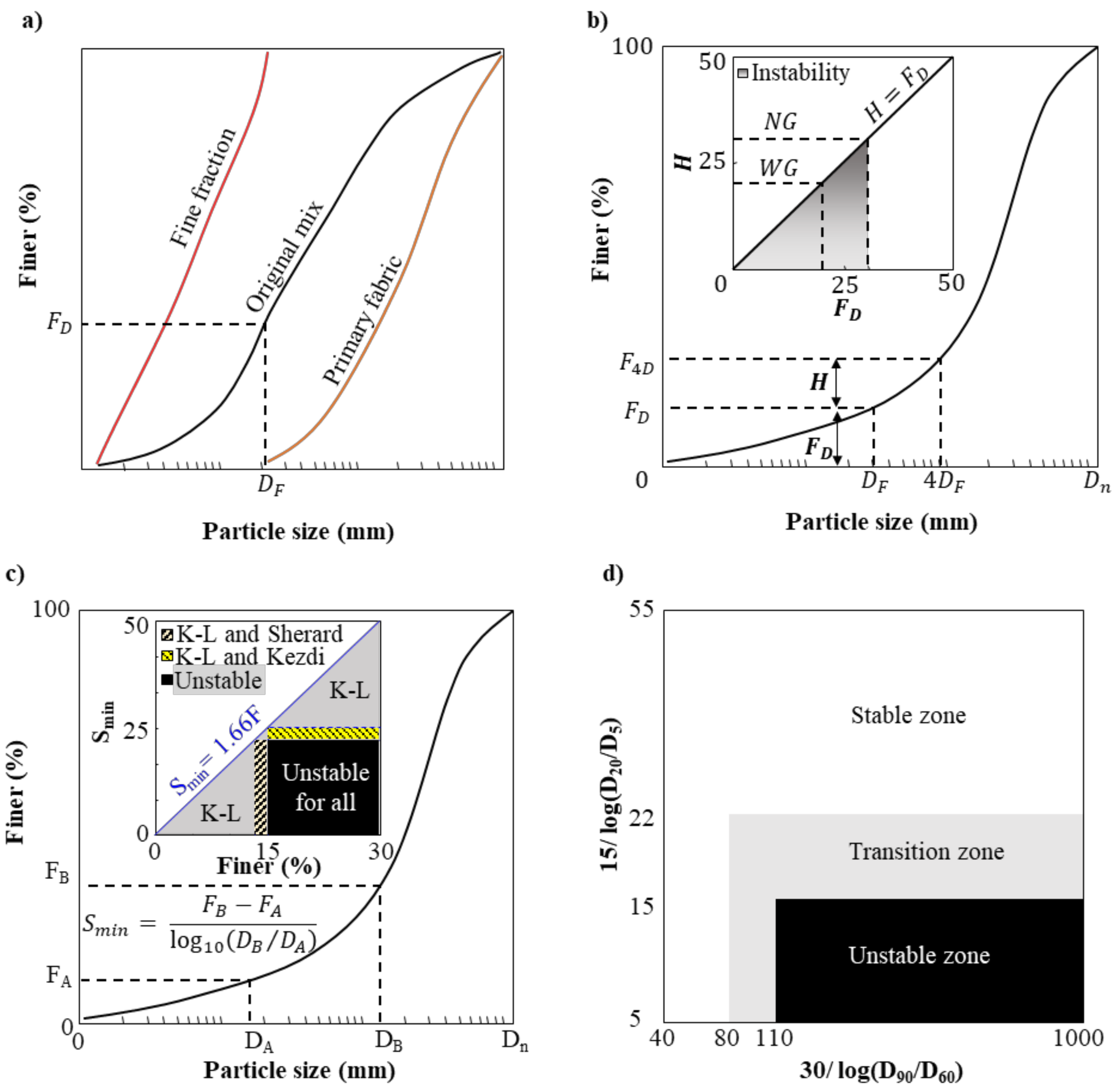

Figure 3. Development of the graphical assessment techniques: a) division of PSD curve of the soil as proposed in [68]; b) Kenney and Lau method [34]; c) Modified internal stability assessment criteria [30]; d) butterfly-wings method developed in [71], here K-L indicates stable according to Kenney and Lau method.

Table 2 Selected stability criteria.

Basis	Criteria	Source
Size	$d_{\mathrm{F},15} < 0.25 d_{\mathrm{P},15} < d_{\mathrm{F},85}$	[68]—(A)
	$I_r = \left(d_{\mathrm{P},15}/d_{\mathrm{F},85}\right) < 5$	[67]—(B)
	$0.76\, log(h'') + 1 < h' < 1.86\, log(h') + 1$ —stable	[54]
Shape	$(H/F)_{min} \geq 1.0$ —stable	[34]—(C)
	$P_G < 25$ —stable	[72]
	$25 \leq P_G < 35$ —transition state	
	$P_G > 35$ —unstable	
Modified	$i_{fine} = 15/\log_{10}(d_{20}/d_5)$;	[30]
	$i_{coarse} = 30/\log_{10}(d_{90}/d_{60})$	
	$i_{fine} \geq 22$ and $i_{coarse} \leq 80$ —stable	
	$i_{fine} \leq 15$ and $i_{coarse} \geq 110$ —unstable	
	for $F < 15$: $(H/F)_{min} \geq 1.0$ —stable	[29]
	for $F > 15$: $H \geq 15$ —stable	
	$P_f < 10$ and $G_r < 3.0$ —stable	[42]
	$10 \leq P_f \leq 35$ and $G_r < 0.3P_f$—stable	
	$P_f > 35$ —stable	
	$S = (f(4d) - f(d))/(\log 4d - \log d)$: for (C)	[71]
	$S = 15/(\log[f^{-1}(15 + 0.85P)] - \log[f^{-1}(0.85P)])$: for (A and B)	
	$S < 1.66F$ — stable	

P_G: mass (%) passing at the gap location for gap graded soils; d_x(mm): grain size at x% mass passing; P_f: clay and silt percentage by mass (%); $P = f\ (d)$ is the inverse function of the PSD; F: the percent finer (%) value of PSD by mass

A graphical method-also termed as the "grading stability" criterion has been proposed to assess the internal instability of non-cohesive soils using a ratio between two mass fractions [34]. In this method, the mass fraction, $\mathrm{F_D}$, that corresponds to the particle size $\mathrm{D_F}$, is selected from the PSD as the fines fraction. It was empirically shown that the maximum value for $\mathrm{F_D}$ in the case of well-graded soils and 30% for uniformly graded soils (Figure 3b). The mass fraction between the particle sizes $\mathrm{D_F}$ and $\mathrm{4D_F}$ is hypothesised as the determining size range. If the fraction, $(\mathrm{H/F_D})_{\mathrm{min}}$, defined as the stability index, is equal or greater than 1 the soil is identified as internally stable. Here, the mass fraction of the determining size range is large enough to generate finer constrictions allowing the soil mass to filter (or clog) its own migrating fines fraction (self-filtration). A longer or flatter fines tail of the PSD indicates a smaller stability index, and less capability for self-filtration, which is often the problem associated with gap-graded soils with a long tale of fines. In developing the grading stability method, [34] considered an index referred to as hydrodynamic number ($\mathrm{R' = qD_5/\nu n}$). This index is a function of the unit flux (q), particle size ($\mathrm{D_5}$) representing 5% finer by mass of the cumulative PSD, porosity (n) and the kinematic viscosity (ν) of water at a given temperature. The grading stability method was developed under extreme values of $\mathrm{R'}(\geq 10)$ while applying vibrations to the samples to accelerate the migration of fines.

Chapuis [73] employed the secant slope (S), which is the secant value of the angle created by the semilog-PSD between determining particle sizes, to better understand Kezdi [68], Sherard [67] and Kenney and Lau [34] methods. According to Chapuis-generalization [73], Kezdi-method [68] can only identify the internal instability in soils if S values between two log cycles differ by 24.9% (or more). If this difference is 21.5% (or more) Sherard method [67] would indicate internal instability. Similarly, the grading stability criterion would identify a soil as stable if at any given particle size $\mathrm{D_F}$ ($\mathrm{F_D}$<20%), if $\mathrm{S < 1.66F_D}$. This method was modified using the S at different mass fractions (10% increments) [74]. In this attempt, they evaluated a large database of soil PSDs, which were examined for internal stability by previous researchers (e.g. [30], [34]), using the graphical methods and secant-slope method. It was shown that, with statistically significant accuracy, a majority of different PSDs of soils can be segmented into two classes—stability and instability—using a butterfly-wings chart (Figure 3d). This butterfly-wings chart indicates a zone of inconsistency where different methods, such as Kenney and Lau method [34] and Sherard method [67], indicate internal stability for soils that are deemed unstable by other methods.

Since the S values are taken from the discrete points of PSD, this inconsistency is a result of different shapes of the PSDs [71]. Therefore, the method proposed in [74] was extended with a software code to develop the butterfly-wings chart using the statistically best-fit curve of the soil PSD. In this method, the PSD curve is estimated as the inverse function of the percent finer by mass, which could be differentiated to get the minimum secant slope S_{min} at any mass fraction increment. This technique addresses the problem of differently shaped PSDs while improving the potential for developing the secant-slope based method as a universally applicable assessment method. However, grading stability method proposed in [34] has been, still, preferred by most of the practicing engineers as a rule of thumb due to its high consistency in predicting internal stability compared to other conventional methods.

Apart from a few studies, such as [54], [75], and [30], limited number of key studies have attempted to evaluate the internal stability of cohesive soils or gap-graded soils. Burenkova [54] developed a criterion that could be applied to gap-graded cohesive soils. This method employs a set of particle size ratios, known as conditional factors of uniformity, h' ($\mathrm{h}' = \mathrm{d}_{90}/\mathrm{d}_{15}$) and h''($\mathrm{h}'' = \mathrm{d}_{90}/\mathrm{d}_{60}$). The region for internal stability has been graphically defined by plotting h' vs log (h''). However, this method employs dry mixing of soil mixtures. Therefore, its applicability in assessing the seepage induced internal instability in soils requires further investigations. Wan and Fell [30] reproduced the test results of the earlier studies using consistent hydro-dynamic conditions (R' values) to compare the applicability of stability criteria developed for non-cohesive soils to cohesive soils. They introduced a modified method to estimate the internal stability of widely graded silt-sand-gravel soils with plastic fines (Figure 3d). Moreover, they showed that the method proposed by Kenney and Lau [34] underestimated the internal stability at values of $F_D > 15\%$ since the soils that were deemed unstable stabilized and showed no erosion state with very little loss of fines. Additionally, Li and Fannin [75] showed that Kezdi [68] method was more conservative in estimating internal stability of soils when $F_D < 15\%$. Also, Li and Fannin [75] emphasized that, compared to these two methods, the method proposed by Burenkova [54] remained less conservative for all the tested soils. Collectively, all of these methods show inconsistencies in evaluating gap-graded soils with high fines content to be internally unstable. The estimations overlook the potential self-filtration capacity of soils with high percentage of fines. As shown in Figure 4a to c, when the fines content is high, the soil matrix becomes fines dominant [76]. Thus, the coarse particles "float" in the fines, which can lead to a transitional relative density where fines also play a major role in transferring the applied stresses in the soil matrix. Assessing internal instability in this type of soils become extremely challenging. For such soils, Chang and Zhang [77] were the first to propose that the fines percentage should be included together with the size of the gap in PSD to predict the soil internal instability.

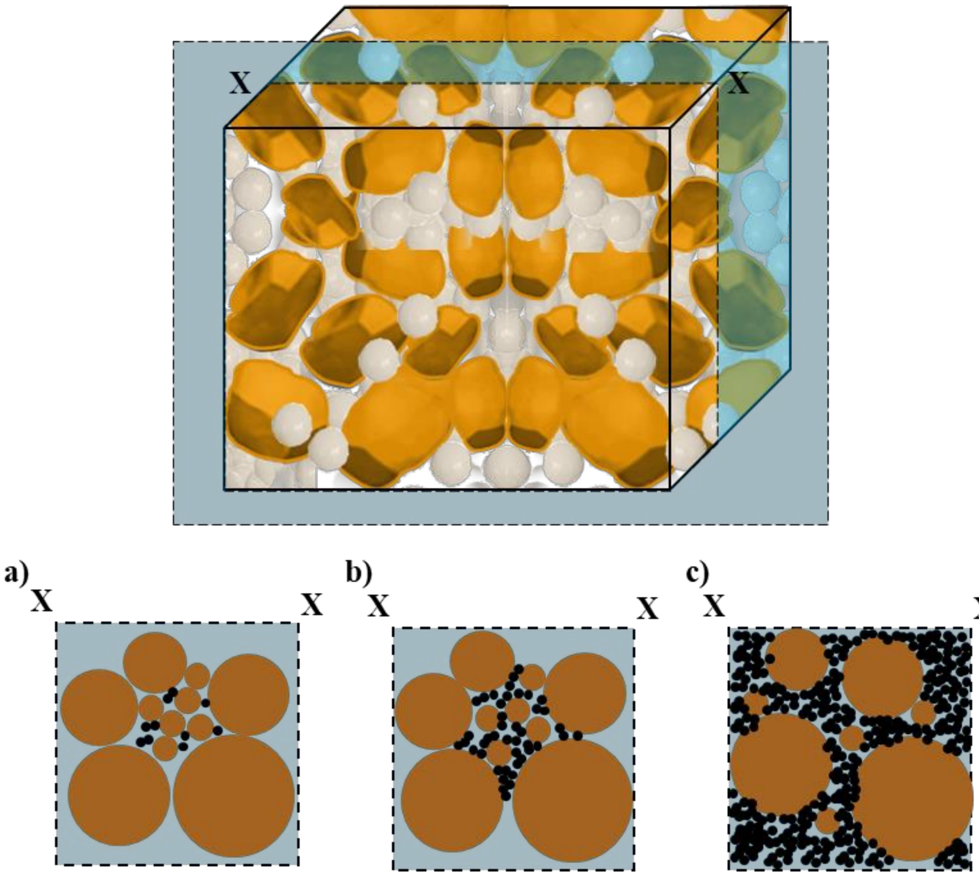

Figure 4. Soil matrix at different fines percentages: a) less than 10%; b) between 10 to 35%; c) more than 35% (after [76 and 77]).

To estimate the relative difference of maximum (D_{min}) and minimum (d_{max}) particle sizes of the gap, the authors in Chang and Zhang [77] introduced an index ratio: the gap-ratio ($G_r = D_{min}/d_{max}$). The G_r value can be used together with the fines percentage to predict the internal instability of soils with higher fines content typically exceeding 30% [77]. Compared to the earlier graphical methods, including [34], this method provided a paradigm shift to the internal stability assessment in soils with high fines content.

As shown in Figure 5, a data base of particle sizes in the PSDs used to define most of the widely available geometric criteria was developed from the literature cited in this paper. It is clear that the PSDs in the literature have limited variability of the particle sizes beyond the size range of fine gravel. There are apparent gaps between the sizes of D_{20} and D_{10} and D_{60} and D_{20} values, in the case of internally unstable soils. In the context of internally stable soil PSDs, only the D_{20} and D_{60} are located apart. The two gaps for the case of internally unstable soils indicate either a gap or a broad size distribution in their PSDs. However, it should be noted that the internal instability of all of these PSDs have been studied under different experimental conditions.

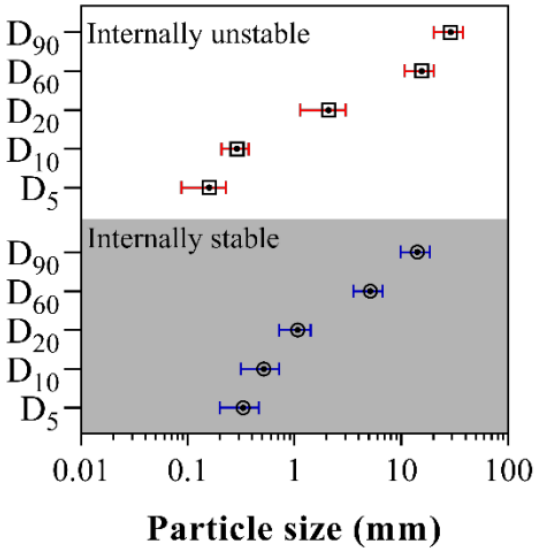

Figure 5. The distribution of the tested grain sizes in the PSDs from the cited literature

Most of the conventional geometric criteria have been developed as design guidelines to assess the internal instability of soils under extreme hydraulic gradients (values exceeding 10). Hydraulic structures do not typically experience such extremity in their service lives [78, 79]. Therefore, the classical criteria tend to underestimate the internal stability of soils under normal operating conditions, and hence provide conservative measures.

3.3. Analytical methods

The statistical and probabilistic theories employed to model the transport of fines through the pore network hypothesise that the load bearing primary fabric is a collection of sieves with random aperture sizes representing constrictions. In these models, irregular, or sub-angular soil particles are assumed to be frictionless spheres, and the 2-D cross-section of a particle assembly is taken to represent the hypothetical sieve. The aperture size of this hypothetical sieve represents a constriction, which is the size of the window between two adjacent pores at a given location. Thus, the conventional PSD based assessment of internal stability is replaced with the instrumental notion of constriction size distribution (CSD) of the primary fabric. If soil particles are idealised as spheres, the PSD could be hypothesised as the cumulative probability distribution of the respective particle sizes [80, 81]. The percent finer by mass for a given particle size d_i, denoted as P_{d_i}, conceptually represents the probability of detecting the particle smaller than this size. Holding this probabilistic perspective, the fraction of the PSD belonging to primary fabric can be discretized into finite regions (Figure 6a), which could be attributed with the mean particle diameters (d_i) and representative mass fractions (P_{d_i}). Using two dimensional projections of the particle arrangement the constriction sizes in between the particles can be geometrically estimated. As shown in Figure 6b, the arrangement of three different particle (d_1, d_2, and d_3) all in contact forms the smallest constriction size $(D_c)_3$, which, for the first time for soils, [80] expressed mathematically as follows (Equation 1):

$$(D_c)_3 = \frac{\mathrm{d_1 d_2 d_3}}{\mathrm{d_1 d_2 + d_1 d_2 + d_1 d_2} + 2\sqrt{\mathrm{d_1 d_2 d_3 (d_1 + d_2 + d_3)}}} \tag{1}$$

For the constriction sizes in the looser particle packing, a two-dimensional model considering four particle diameters (d_1, d_2, d_3, and d_4) (Figure 6c) was proposed [80]. In this model the area of the inscribed constriction (S_c) was expressed as:

$$S_c = \frac{1}{8}\left[f(\alpha) + f(\gamma) - \left(\alpha \mathrm{d_1}^2 + \beta \mathrm{d_2}^2 + \delta \mathrm{d_3}^2 + \gamma \mathrm{d_4}^2\right)\right] \tag{2}$$

where $f(\alpha) = (\mathrm{d_1+d_2})(\mathrm{d_1+d_4}) \sin\alpha$, and $f(\gamma) = (\mathrm{d_2+d_3})(\mathrm{d_2+d_4}) \sin\gamma$.

This model includes the internal angles (α, β, δ, and γ) measured in radians. At the loosest packing, four particles form the maximum constriction area ($(S_c)_{max}$) expressed as:

$$(D_c)_4 = 2\sqrt{\left(\frac{(S_c)_{max}}{\pi}\right)} \tag{3}$$

In an alternative method, the value of the angle α in Equation 2 can be changed from the smallest to the largest possible angle to account for the density variations in calculating $(D_c)_4$. Up-to-date, despite the lack of experimental validations for both of these techniques, a majority of studies still employs them to analytically estimate the minimum and maximum constriction sizes (e.g. [82], [83], [33]). To the benefit of this concept, experimental studies on other research domains, such as magnetic resonance imaging, have shown that pores are typically formed by four particle arrangements [84]. In addition, Scheuermann and Bieberstein [84] have developed an analytical model for the soil water characteristic curve using the constriction sizes obtained by changing the inscribing angles in Equation 2. The experimentally obtained soil water characteristic curve shows a close resemblence to the constriction size estimation derived from the analytical model. On the contrary, the numerical simulations at the particle scale have show that these idealized configurations rarely occur even in samples with linear PSDs [85].

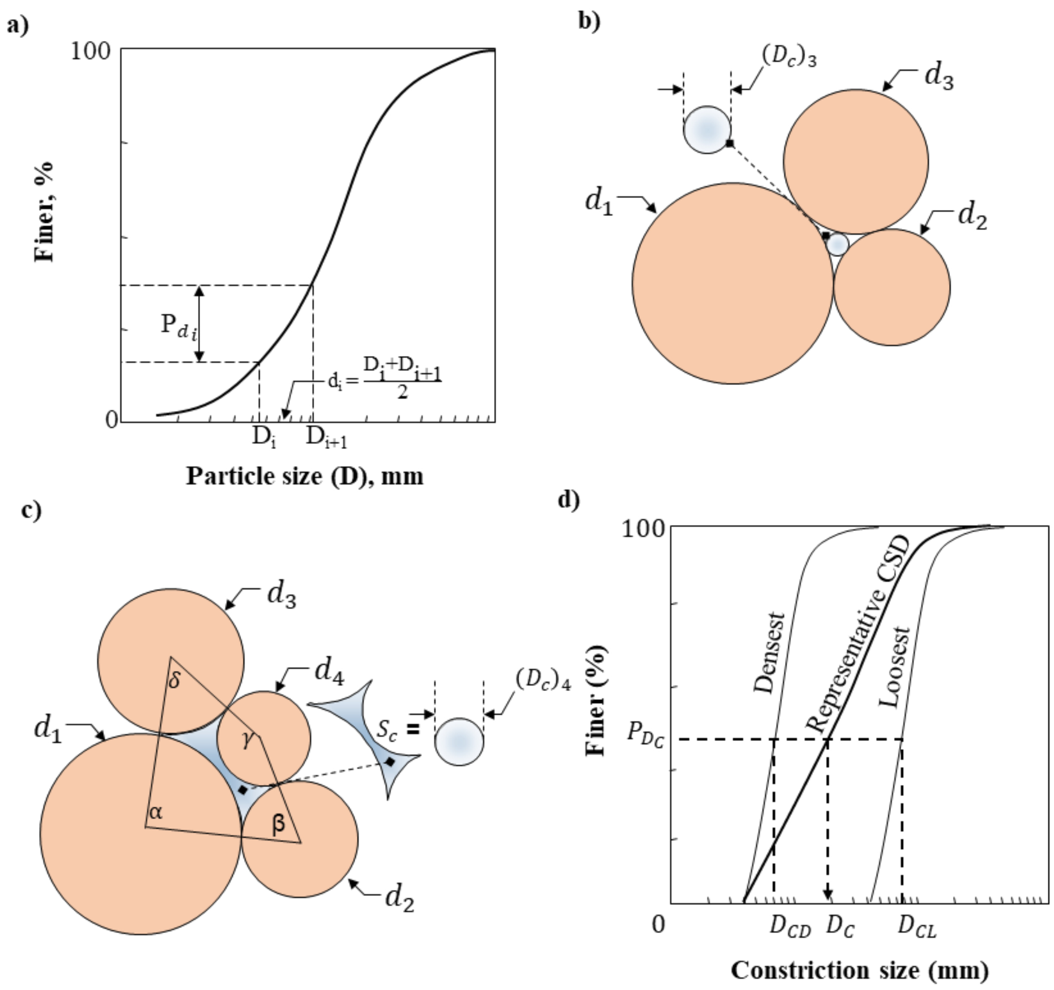

Figure 6. Constriction size distribution (CSD): a) the discretisation of the PSD; b) cross section for three particle arrangement for the densest state; c) cross section for four particle arrangement for the loosest state; d) representative CSD of the idealised soil sample.

Humes [86] provided probabilistic expressions for the probability of occurrence (P_C) of the previously estimated constriction sizes in 3 and 4 particle arrangements (Figure 6b and c) respectively. In these arrangements, the total number of occurrence ($\sum n_i$) of given particle diameters (d_i) should be always equal to 3 or 4 for densest and loosest states, respectively (Equation 4).

$$P_C = \begin{cases} \frac{3!}{n_1 n_2 n_3}\left(P_{d_1}\right)^{n_1}\left(P_{d_2}\right)^{n_2}\left(P_{d_3}\right)^{n_3}; for\ n_1 + n_2 + n_3 = 3 \\ \\ \frac{4!}{n_1 n_2 n_3 n_4}\left(P_{d_1}\right)^{n_1}\left(P_{d_2}\right)^{n_2}\left(P_{d_3}\right)^{n_3}\left(P_{d_4}\right)^{n_4}; for\ n_1 + n_2 + n_3 + n_4 = 4 \end{cases} \qquad (4)$$

The coarse particles in a discrete PSD size interval, typically part of the primary fabric, yield a higher mass fraction compared to the finer particles. Therefore, the occurrence probabilities calculated based on the PSD by mass can overestimate the number of larger constrictions in well-graded soils [86]. For those soils, C_u increases with the presence of more small particles to fill the larger pores. This filling increases the number of narrow size constrictions and, subsequently, the number of particles proportionately increases the avail- able surface area for particle contacts. Therefore, as proposed in [86], that this over-representation of larger constrictions should be addressed by estimating the surface area distribution (Equation 5). However, the surface area distribution cannot represent the number of particles that would result in the constriction sizes through particle-to-particle contacts. Hence, Raut [87] developed the equation to calculate the particle distribution by number of particles (Equation 6).

$$(P_S)_i = \frac{P_{d_i}/d_i}{\sum_{i=1}^{n} P_{d_i}/d_i} \tag{5}$$

$$(P_N)_i = \frac{P_{d_i}/{d_i}^3}{\sum_{i=1}^{n} P_{d_i}/{d_i}^3} \tag{6}$$

where $(P_S)_i$ and $(P_N)_i$ indicate the probability of occurrence based on the contact surface area and number of particles, respectively.

The maximum and the minimum densities in the primary fabric represent the two extreme states of packing: the minimum void ratio (e_{min}) and the maximum void ratio (e_{max}), respectively. The relative density (R_d) for any particle packing in between (e) is a measure of how far the current density is from these two limits. As such, it has been hypothesized that the constriction size D_C should be linearly dependent on R_d [88] (Equation 7):

$$D_C = D_{CD} + P_{D_C}(1 - R_d)(D_{CL} - D_{CD})\ ;\ R_d = \frac{(e_{max} - e)}{(e_{max} - e_{min})} \times 100 \tag{7}$$

where D_{CD} and D_{CL} are the constriction sizes in the maximum and the minimum density arrangements of three and four particles respectively, (see Figure 6b and c). In this context, P_{D_C} expresses the cumulative percentage of constrictions at an arbitrary group of particles. Analogous to PSD, the cumulative distribution of D_c values represent the CSD of the primary fabric at a given R_d (Figure 6d).

Studies presented in [80] and [89] were the earliest to propose that fine particles followed linear trajectories (Figure 7a) parallel to a unidirectional hydraulic flow through the constriction network. The migrating fines would encounter random constrictions along these unidirectional trajectories. The passing probability (P) for the particle can be identified as the cumulative probability of subsequently encountering constrictions larger than the particle size (d) until a constriction of a smaller size ($D_C < d$) obstructs its movement. Equation 8 shows the number of confrontations (N) until a particle encounters a constriction smaller than d. This value was earlier experimentally found in [90] and recently endorsed by [88] and [91] using both experimental and analytical techniques. Some authors have adopted a value of 98% for P (e.g. [90]), whereas others have suggested a statistically significant value of 95% (e.g. [88]).

$$N = \frac{\ln(1-P')}{\ln(P)} \tag{8}$$

where, P' is the confidence level. The depth of infiltration ($L = N.s$) is calculated from the thickness or the unit step (Figure 7b) of the layer (s), which lies in the size range of $D_5 - D_{10}$ for cohesionless granular soils [88].

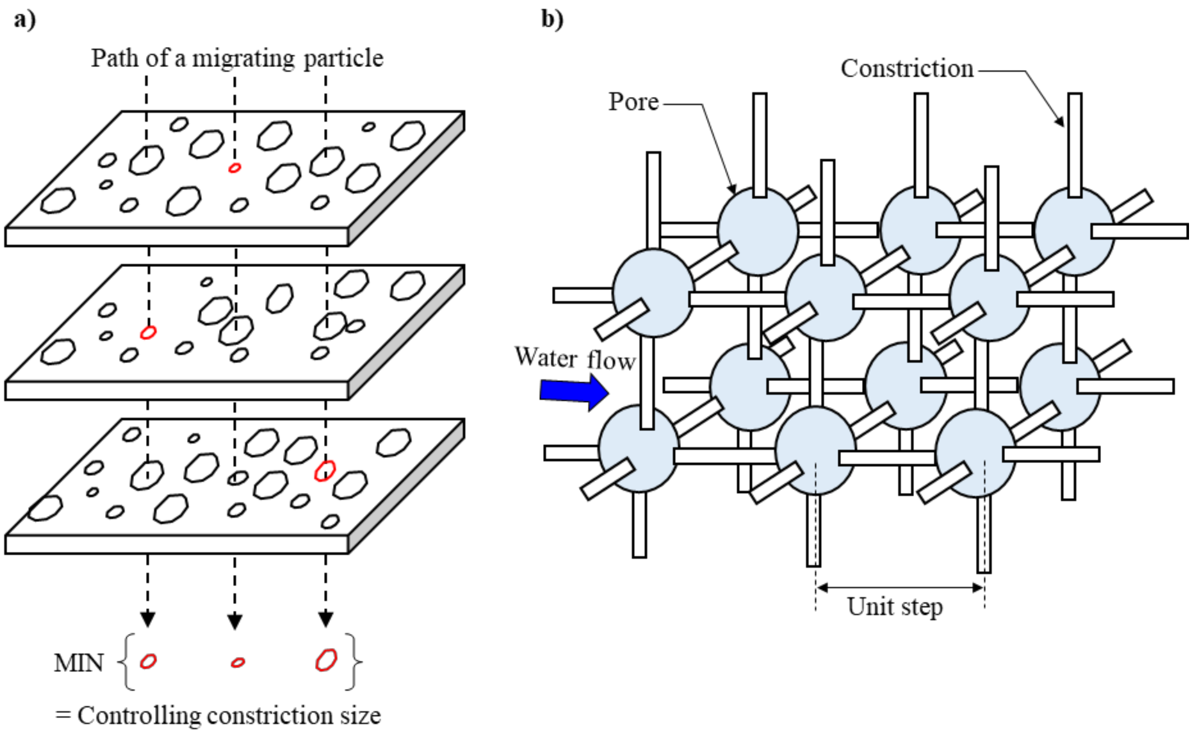

Figure 7. Probabilistic particle transport concept: a) controlling constriction size in unit layers; reproduced from [32]. b) cubic pore network model; reproduced from [25] with permission from Journal of Geotechnical and Geoenvironmental Engineering.

3.4. Summary of classical approaches

In view of the presented methods and approaches, conventional assessments of internal instability relies on idealised experiments – often they are associated with empirical propositions that are yet to be fully validated. Potential internal instability of granular soils is typically based on selected shapes of the PSDs (Figure 8). Most of the studies were performed using constituted granular soils rather than the samples taken from the field. They have been subjected to extreme hydraulic conditions to define the classical stability criteria, which are based on size ratio, PSD shape and slope, and the unified (or normalised) forms. Analytical models are possible only because of the experimental observations and the empirical realisation of the soil instability phenomenon. The notion of controlling constriction size has been mathematically modelled using computational geometry and probability theory, however, with little physical evidence or experimental support.

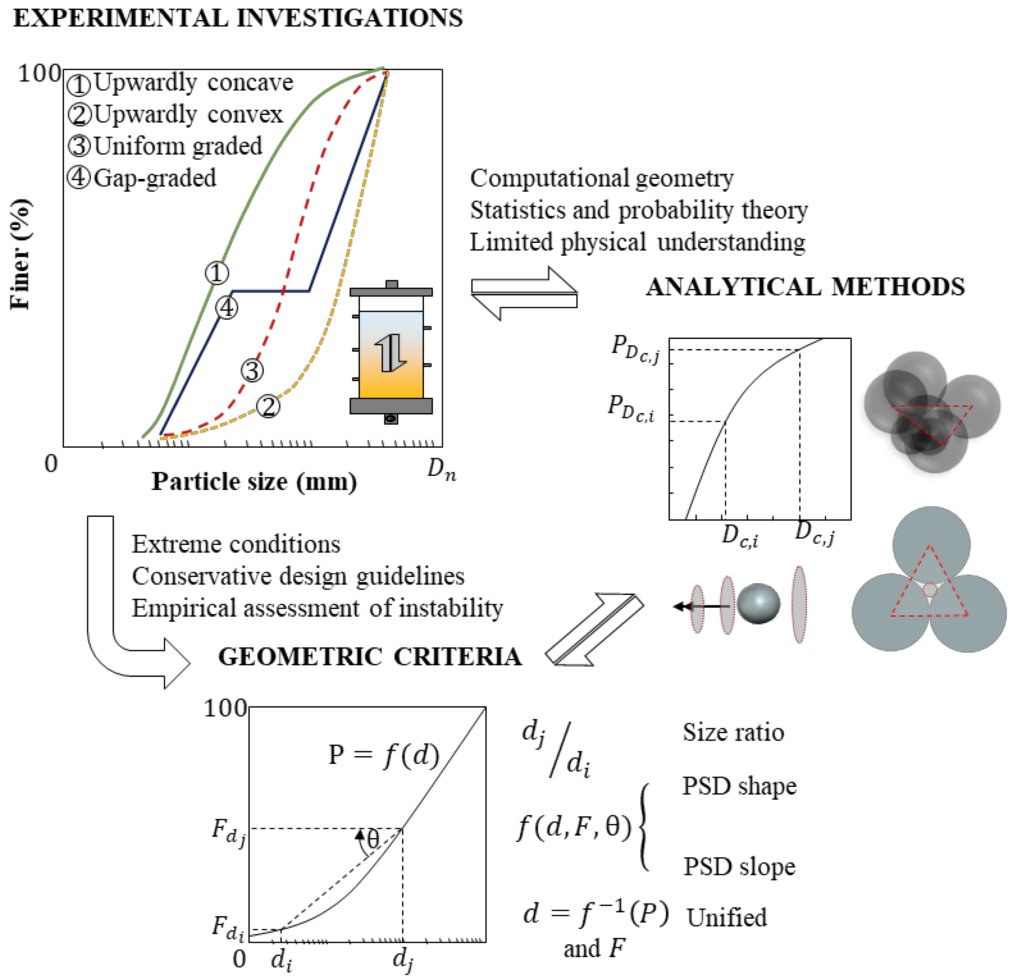

Figure 8. Classical knowledge and methodologies used for assessment of internal instability.

Geometrical assessment techniques have evolved to become common practical design guidelines for internal stability in dam engineering [92]. They appear to evaluate the internal instability potential of various types of soils with accept- able accuracy. Their success is backed up by the basic laboratory tests. The experimental methods employed in defining them typically disregard actual hydrodynamic conditions. They are in essence accelerated experiments intended to provide a conservative assessment of soil's internal instability. Given the lack of information reported in literature, the accuracy of the geometric criteria on evaluating different soil types need to be re-examined. The wide array of experimental conditions found in the amassed literature is reflective of lack of consensus on the range of fundamental parameters affecting internal instability.

To date analytical methods used are mathematical and statistical expressions for the internal instability of a collection of frictionless spherical particles. Constriction network or probability of fines transport through such idealised particulate assemblies are significantly different from those in natural porous media, where tortuosity and particle's surface friction undoubtedly affect the particle migration. The lack of experimental validation for these analytical methods coupled with the limited knowledge on the underlying mechanics of the phenomenon challenge their applicability in many geo-applications. Perhaps, a possible validation of such methods may come through improved physical modelling and theoretical realization in the future. Furthermore, to complement the numerical simulations, pore size distribution and CSD need to be accurately mapped for a better representation of the particle migration paths. To this end, developing more advanced experimental technologies for monitoring particle migration and extremely efficient algorithms for simulating their movements are instrumental.

4. Recent developments

Technological development in the new millennium has opened up new horizons for exploring fundamental micro-scale mechanics of the internal instability phenomenon. It has made numerical techniques, such as discrete element method (DEM) (e.g. [93]), that simulate micro level particle interaction feasible, and visualisation of the particle migration possible through non-invasive monitoring techniques, such as X-ray microtomography and neutron tomography (e.g. [94], [95]).

The improved experimental technologies have warranted different researchers to provide new insights into the mechanics of internal instability phenomenon.

4.1. Methods based on DEM simulations

The movement of particles at the microscale can be numerically simulated applying Newtonian mechanics to each particle and mapping their respective positions for each time increment [93, 96]. These simulations, typically called discrete element method simulations or DEM, use a collection of discrete spherical particles to represent soil grains. From the perspective of revealing the underlying mechanics of internal instability phenomenon, computational techniques based on the DEM have been more popular and convenient with the robustness of recent hardware [97]. For instance, [98] employed DEM techniques to quantify the internal force chains developed in particle packings, and hence the load bearing fabric. Also, other researchers have utilized the DEM generated data for inverse statistical modelling of internal instability (e.g. [83]). However, the simulation of the complex 3-D pore structure of the soil packings has been the most general application of DEM (e.g. [82], [99], [100]).

Fundamentally, in DEM, the evolution of the bulk mechanical properties of a particle assembly depends on two parameters: the geometry of the particles and the interaction forces between them. A contact between two particles is defined when they share a common volume (or an overlapping zone) in the assembly (Figure 9a). The connection is mechanically modelled as a link created by two fictitious linear springs and a slider (Figure 9b).

In the mechanical representation, the contact normal stiffness (k_n) of given two particles is defined as proportional to the harmonic mean of the two radii. As given in Equation 9, the proportionality constant equals the Young modulus (E) of the material [101]. Moreover, the tangential stiffness (k_{tang}) is a fraction of its normal counterpart (Equation 10). The ratio is called the stiffness ratio (α_n).

$$k_n = \frac{E(D_{\mathrm{p1}} \times D_{\mathrm{p2}})}{(D_{\mathrm{p1}} + D_{\mathrm{p2}})} \tag{9}$$

$$\frac{k_{tang}}{k_n} = \alpha_n \tag{10}$$

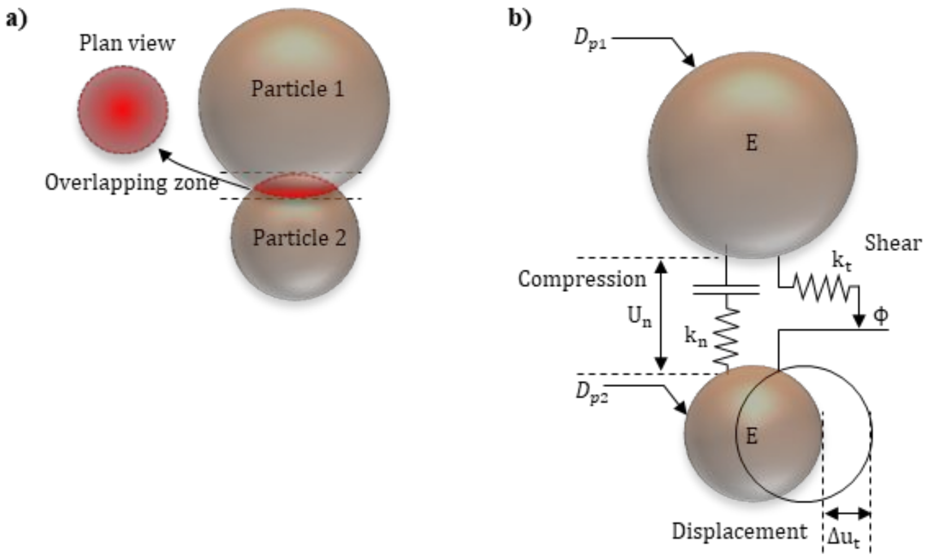

Figure 9. Elements of DEM simulations: a) overlapping particle contact model; b) representative mechanical model for particle contact.

The normal force (F_n) acting along the direction of the vector joining the particle centres is proportionate to the normal overlapping distance (U_n) between the two particles [102]. The contact normal stiffness acts as the linear proportionality constant (Equation 11).

$$F_n = k_n U_n \tag{11}$$

Similarly, the tangential force (F_t) is proportionate to tangential displacement (Δu_t) where the proportionality constant equals k_{tang} (Equation 12). Moreover, the maximum possible value for the ratio between normal and tangential forces equals the internal friction angle (ϕ) of the material (Equation 13). This ratio follows a linear trend as long as the Coulomb friction condition is assumed [102].

$$F_t = k_{tang} \Delta u_t \tag{12}$$

$$\left(\frac{F_t}{F_n}\right)_{max} = \phi \quad (13)$$

Restrained by the objective functions given in Equation 9 to 13, the particle displacement and resulting internal forces, can be computed using the position coordinates of the particles. This simple computational procedure can be integrated to model millions of possible combinations of the particle arrangements and the resulting CSDs (e.g. [82, 99, 100]).

The internal pore structure of the particle packings has been developed mostly using two techniques: the Delaunay method and the Voronoi method [82, 94]. In the Delaunay method, the constriction size is represented by the largest disk that can fit on the surface of the tetrahedron whose corners are connected to the centres of four different spherical particles [99, 100]. In this manner, tessellating the 3-D particle assembly with discretised tetrahedrons yields a distribution representing the number and size of constrictions: CSD. In the Voronoi method, random points are distributed in the pore space of an assembly of spherical particles. The nearest distance to the solid spherical particles from the randomly distributed points are considered to be equal to radii of open spaces [103]. The larger radii represent the pores, while the smaller radii represent the constrictions. Both of these methods require extremely high computational power. In the case of well-graded PSDs, Delaunay 3-D tessellation results in a large number of tetrahedrons and evaluates the pores as constrictions [82, 103]. This is a result of the wide range of constriction sizes, and it can be resolved by adjusting the resolution of the 3-D tessellation (i.e., tetrahedron size). On the other hand, Voronoi algorithm can successfully address this issue since it only uses the distance from random points to compute the constriction network and it is independent of the resolution of the 3-D tessellation.

DEM techniques have shown that some particles considered to be a part of the fines fraction appear to transfer the applied stresses, and they are part of the force chains [81, 104]. The size of these particles cannot be identified using the PSDs alone, they belong to both the primary fabric and fines fraction (i.e., an overlapping zone) [81]. The particles in the overlapping zone of the PSD carry the applied stresses because of the particle- to-particle friction [105]. The inter-particle frictional forces are excluded in the conventional analytical methods by the idealisation of the soil particles as perfect frictionless spheres, and they fail to identify the overlapping zone. CSDs generated by DEM methods that include particle-to-particle friction show that the analytical methods overestimate constriction sizes for well-graded PSDs. The finer particles in such PSDs can also contribute to the overlapping zone and form an increased number of finer constrictions [105]. Continuous loss of the load bearing finer particles in the overlapping zone could distort the sample and reduce its volume. This realisation of an overlapping zone could underpin the transitional nature of suffusion to suffosion.

The suffusion (or suffosion) process causes the transitional behavior of binary mixtures (i.e., gap-graded mixtures) by altering their coarse to fine particles mixture ratio [106]. Typically, the subtle and erratic changes of these transitional properties have been quantified using behavioral thresholds that include the generalized state parameters and/or effective properties, such as the density, normalized density, and volume fraction of each component of the binary mixtures [107, 108, 109, 110, 153]. For instance, it has been suggested that sand-fraction percolation results in a tendency to volume-change (analogous to suffosion) in mixtures of sand and clay subjected to undrained tri-axial shear [106]. Moreover, an empirical study on developing optimal seepage-barrier materials showed that the compressibility and conductivity of mixtures were strongly influenced by the course to fine mixture ratio [112]. The studies on soft-rigid binary mixtures show that the fraction of the soft particles governs the percolation network, particle structure, stress network, and local void developed by the rigid particles by preventing the buckling of rigid particle chains [113, 114]. To maintain the skeleton, the optimum range of the rigid fraction should lie between 60-80%, and beyond this range, the primary fabric deformation dramatically increases [113]. However, the percolation of real three-dimensional polydisperse assemblies of binary mixtures (such as coarse particles in a fine matrix) has not been comprehensively understood up-to-date.

The DEM simulations can be employed to overcome the experimental challenges in visualising the particle migration occurring at the micro-level. This also provides a feasible alternative for the costly and lengthy experimental programs (e.g., neutron tomography) involving in the visualization of the pore network [103]. DEM approaches can be successfully used as an effective tool for fundamental investigation of the microscopic mechanics of the internal instability phenomenon [115]. However, still, the numerical techniques that hypothesise soil as a collection of discrete particles require theoretical and computational improvements to simulate the variations of macro-level properties, such as strength and hydraulic conductivity, resulting from the particle migration at the micro-scale. Compared to the earliest attempts of DEM (proposed in [116]), the more recent computational capabilities, such as the combined DEM-Finite element method (DEM-FEM) (e.g. [97]), allow integrating the DEM methods into large-scale models.

4.2. Non-invasive monitoring techniques

Modern experimental visualisation techniques, such as particle image velocimetry (PIV) and positron emission particle tracking (PEPT) [117, 118], provide an efficient vehicle for visual monitoring of the internal instability phenomenon. Particle migration in opaque granular systems can be traced during a flow test using these particle tracing methods, and the traced migration paths can be employed to model the migration phenomenon as a temporal function [119]. For accurate visualisation of the flow distribution, the neutrally buoyant hydrophilic tracer particles should be thoroughly mixed and suspended in the fluid to obtain an identical velocity field to that of fluid flow field [120, 121]. It is critical to note that these methods could trace the migrating paths of the fine particles only when a fixed-part of the particle fabric remains intact and stationary. As such, the primary fabric and the fines fraction need to be accurately defined, and the tracer particles should belong to the migrating fines fraction. If the soil fabric is going to collapse, as in the case of suffosion, the particle tracking yields inaccurate results during the experiment since the fines and primary fabric could migrate together with the tracing particles. As such, monitoring the occurrence and progression of internal instability would be extremely challenging.

The inherent limitations of the visual techniques are the opaque nature of the soil specimen and the difficulty in capturing the particle migration at a depth beyond the permeameter wall. Some studies have attempted to overcome these limitations by using modified samples and permeants. Rosenbrand and Dijkstra [122] used artificially coloured sand particles mixed as tracers to visualise the migration in sandy gravel soils. These dyed sand particles have different shapes compared to the particles forming the fines fraction. Their unit weight is slightly higher than that of the fines fraction (27 kN/m^3). The higher weight is expected to cause slower flow and settlement of the dyed particles compared to the mobile fines. In a similar experiment, optically matched (identical refractive indices) oil mixed with the fluorescent dye was used as a substitute to water to observe the movement of glass particles [123]. They used fractured pieces of glass to represent the angularity of the natural soil particles and employed plane laser induced fluorescence (PLIF) technique to illuminate the fluorescent dye. At the initiation of particle suffusion, their results indicate a considerable change in specimen volume in addition to the very low hydraulic gradients (around $i = 0.25$). The observations also flag the existence of an overlapping zone, as described in the preceding section, and it is evident that the suffusion leads to suffosion when the fine fraction of the soil also carry the applied stresses [123]. The plane on which the particles move could be fundamentally observed because of two reasons: the transparency of the sample and PLIF technique. Further research should be carried out on developing transparent soil samples, which are identical to natural soil, and inducing similar physico-chemical properties to the permeant oil and dye to merit from visualization techniques such as PLIF technique.

X-ray computed tomography (X-ray CT) and microtomography (micro-CT) are presently the most popular non-invasive visualisation techniques to capture the pore structure in porous media (e.g. [94],

[124], [125]). The principle of this method is the variation in local densities and structure of a soil assembly, which induces attenuations in the passing X-ray beam energy. The CT scanners (either medical or industrial) typically produce X-ray (electromagnetic radiation) by applying a high voltage between an anode and a cathode made from high atomic weight materials (e.g. platinum or tungsten). The high voltage applied across these electrodes consequently generates a beam of accelerated electrons (cathode rays). When these accelerated electrons are decelerated at the anode, a beam of X-rays is generated. If this X-ray beam is allowed to penetrate through a homogeneous sample, a portion of the primary beam is absorbed or scattered out of the beam: a phenomenon known as X-ray attenuation.

As given in Equation 14, Lambert–Beer's law describes the intensity of transmitted radiation I and the intensity of incident radiation I_o to the material [126].

$$I = I_o e^{-\mu_a x} \tag{14}$$

where x is the distance travelled by the X-ray beam through the material, and μ_a is the linear attenuation coefficient of the material. It should be noted that the medical X-ray sources emit polychromatic X-rays consisting of a spectrum of different wavelengths, and the attenuation coefficients can be different for each wavelength. Moreover, the attenuation of an X-ray beam depends on the electron density of the soil, the energy of the radiation, and the bulk density of the sample. However, in practice, single linear value μ_a is assumed as the attenuation coefficient. A detailed discussion on the X-ray sources and their interaction with materials can be found in [127].

From the radiograph generated from this operation, an indexed image is reconstructed. In this image the signal in each point is expressed in dimensionless Hounsfields units using Equation 15 [126].

$$\mathrm{CT} = 1000 \frac{\mu_a - \mu_{a_w}}{\mu_{a_w}} \tag{15}$$

where μ_{a_w} is the attenuation coefficient of pure water. The calibration usually used gives CT=0 for water and CT = -1000 for air. In the image reconstruction phase, the acquired radiographs (often called slices) of the transmitted radiation are stacked according to their acquisition order. The stacked collection of these slices is used to construct the 3D internal structure of the sample. Scanner resolution defines the resolution of these rendered 3D volumes. As such the size range spans from millimetre to sub-millimetre level (particularly in micro-CT images). The slice thickness and the 2D resolution of the sensor defines the voxel size of the acquired CT image.

The 3D volume representation of a CT scan results in a collection of voxels, the 3D equivalent of a 2D pixel. The voxels represent the intensity of the attenuation of X-ray at given locations in the sample in grayscale or colour. In the case of constituted soil samples, the different levels of X-ray attenuation result from the differences in phase densities: air, water and material. When the intensity threshold is known for the material the void and the particle phases can be distinguished. As such, a binary image (or slice) containing material and void, represented as 0 and 1 respectively, can be generated. Once these binary images are developed, the visualization and quantitative analysis that lead to pore network extraction follow a typical image analysis procedure [128].

Two major challenges hinder the development of CT scanning method as a potential visualisation technique to observe internal instability in soils. One is the difficulty in extracting (or preparing) an undisturbed sample before and after the testing. Impregnating the specimens with a resin that preserves the soil structure (minimal shrinkage during curing) is the most widely used technique to counter this; commercially available resins (e.g. EPO-TEK 301) have been effectively used for this purpose (e.g. [129]). The second challenge is the difficulty in monitoring (or mapping) the cluster of migrating fines in real-time. This is often overcome by integrating DEM simulations with micro-CT imagery (e.g. [130]), through statistical inference or machine learning techniques (e.g. [47], [131]). In the DEM simulation-based methods, X-ray images taken at different time intervals are coupled with the numerically calculated deformations and distortions of particle clusters (e.g. 10,000 particles) to interpolate the particle movements of the sample. Here, X-ray images also become experimental validations for the numerical simulations and vice versa.

The use of visualization techniques is comparatively less popular in investigating internal instability, mainly due to the practical difficulties in discerning the primary fabric from the migrating fines fraction. The opaque nature of soils equally poses a greater challenge. X-ray images can only be used to construct the CSD of the soil structure, but they alone cannot be used to map the particle suffusion occurring inside the specimen. Studies that experimentally observe the particle migration used transparent samples/particles or an optically matched permeant fluid other than water [123, 132]. Given the complexity of this phenomenon, it is arguable whether the tracing particles can travel at the same velocity as the migrating particles. Although the applicability of using artificial materials to investigate such a complex physical process is arguable, they can provide instrumental experimental evidence to the internal instability phenomenon in soils at the particle level.

4.3. Hydromechanical assessment

The hydraulic and stress criteria that inherently govern the initiation and progression of internal instability have received little attention in the literature compared to the geometrical assessment of internal instability. Although their relevance on the internal instability has been highlighted in the earlier studies (e.g. [60]), the two parameters, hydraulic gradient and the effective stress, could not be simultaneously measured during the experiments until recently because of the technical challenges (e.g. [133], [134]). While the experimental challenges can be largely attributed to the limited availability of studies, the instrumental importance of a mechanics-based constitutive model in complimenting the empirical understanding of internal instability cannot be overemphasized.

It has been experimentally observed that the threshold hydraulic gradient required to drive fines through the constriction network is lesser than the critical hydraulic gradient (i_c) at which the effective stress of the primary fabric becomes zero. Terzaghi [69] expressed i_c at which the soil liquefies (boils), in terms of the specific gravity (G_s) and void ratio (e) (shown with Equation 16). While performing hydraulic conductivity tests on gravel-sand mixtures, Skempton and Brogan [60] observed that soils tend to boil at a lower hydraulic gradient than i_c. Also, they noticed that the difference between the total stress and the pore water pressure for a given depth of the sample was not zero. This resulted in a positive effective stress indicating the theoretical stability of the soil skeleton. To explain this observation, Skempton and Brogan [60] proposed that a majority of the fine particles (sand) occupied the pore space generated by the coarse skeleton, and they transferred only a fraction of the effective stress. Thus, a reduction factor (α) was proposed to estimate the fraction of the effective stress carried by these fine particles. Following this argument, the critical hydraulic gradient that triggered internal instability (i_c') could be estimated using i_c ($i_c' = \alpha i_c$) [60]. For unstable soils with zero overburden stress, α typically varies from 0.7 to 1.0 depending on the direction of the fluid flow. It has further modified in [61] by incorporating the initial vertical effective stress (σ'_{vm}) applied on the specimen as given in Equation 16.

$$i_c' = \frac{\alpha}{(1-0.5\alpha)}(\sigma'_{vm} + 0.5 i_c) \; ; \; i_c = \frac{G_s-1}{1+e} \qquad (16)$$

Chang and Zhang [42] showed that i_c', the hydraulic gradient at which a particle mobilises, can be considered as the critical gradient of initiation. Based on the micro-scale observations of the soil assembly, two other critical gradients can be defined [42]. These are hydraulic gradient at skeleton-deformation, which leads to suffosion, and the failure hydraulic gradient. Only the pore structure of the primary fabric dictates the initiation hydraulic gradient; however, the skeleton-deformation and failure hydraulic gradients depend on the initial stress state, the applied seepage forces, and the shear strength of the soil [42].

In an attempt to develop such a model, Moffat and Fannin [133] proposed a hydro-mechanical failure boundary (an internal instability envelope) to define the critical hydraulic gradient and effective stress at the point of internal instability. Their notion of internal instability envelope is conceptually similar to the Mohr-Coulomb failure criterion. Analogous to the stress failure path, the notion of hydro-mechanical paths is defined as the histories of the local hydraulic gradients and effective stresses across finite distances of the sample. Using this inception, Moffat and Herrera [135] derived a linear model (Equation 17) to estimate the i_c' at instability for the cohesive soils as a function of the deviatoric stress ($\Delta\sigma'_v$), the internal effective friction angle of soil (ϕ'), the vertical effective stress (σ'_v), unit weights of soil and the water (γ_s and γ_w respectively), the ratio between the fines and the coarse fraction (n_f) and an empirical constant (B).

$$i_c' = B(\sigma'_v \tan\phi' + \Delta\sigma'_v) + n_f \frac{\gamma_s}{\gamma_w} \qquad (17)$$

The model discussed in Moffat and Herrera [135] was developed using a rigid-wall permeameter without considering the effect of confinement stresses. They assumed that the confinement pressure and the deviatoric stress, and hence the effective stress, identically increased. The model was not calibrated for the anisotropic conditions where the effective stress was different from the confining stress. Using a flexible wall permeameter, it has been shown that the critical hydraulic gradient (i_c') for the internal instability increases linearly under isotropic stress conditions [136]. But under anisotropic stress conditions the critical hydraulic gradient (i_c'') deviates from this trend. It increases with increasing effective stress to reach a maximum value and then start declining beyond a certain effective stress. This observation challenges previous experimental results since a majority of them could not physically simulate (or measure) anisotropic stress conditions. The discrepancy between the two critical hydraulic gradients is a result of the local segregation of fines, which occurs at anisotropic stress conditions. The temporal changes in the maximum value of the shear function ($f(\tau_{max})$) provides an empirical factor (Equation 18 and 19) to estimate the i_c'' from the i_c' [136].

$$i_c' = \alpha_1 \frac{\sigma'}{\gamma_w \Delta z} + \alpha_2 \frac{\gamma'}{\gamma_w} \qquad (18)$$

$$i_c'' = f(\tau_{max}) i_c' \quad (19)$$

where α_1 and α_2 are stress reduction factors for the effective stress term and the gravity term, respectively; σ' is the confining effective stress on the specimen at the initiation of internal instability.

In cohesionless granular soils, fine particles migrate with the flow through the pore network or connected voids of the coarser primary fabric. A primary fabric with a higher void ratio inevitably allows a rapid migration of fines (e.g. [91]). Thevanayagam and Mohan [137] introduced the concept of inter-granular void ratio (e_s) to estimate the e of load bearing skeleton (i.e., primary fabric). In this concept, the PSD of the soil is considered to be a superposition of two normal distributions (i.e., bi-modal structure) and the tested soil comprises a random mixture where volume of the fines is entrapped in the voids of the coarse particles. Several authors have empirically estimated e_s using e_{max} of the soil mixture [137, 138]. The notion of e_s allows the possibility of estimating a representative controlling constriction size for the soil mixture. Also, this has been supported by empirical studies, such as [33], where the controlling constriction size of the granular soils has been identified as the 35th percentile of the CSD ($D_{C,35}$). The ratio $D_{C,35}/D_{C,85}$ provides an estimate of internal stability of the soil; when it is lower than 0.73 the soil is stable. If the ratio is above 0.82 the soil is unstable. The range between these two extreme values indicates a transitional stability, which has received a limited attention in soil internal stability literature.

Depending on the size and the cohesiveness of the specimen, the local hydraulic gradients experienced by the sample can vary by several orders of magnitude [64, 139]. Evidently, the potential of a soil to experience suffusion cannot be only quantified by the critical hydraulic gradient. Also, the clogging of mobile fines can result in a decrease of the K [47, 128, 140]. In both [141] and [142], the authors attempted to develop a coupled equation for the hydraulic shear stress (τ) developed at a suffusion event. To this end, they employed the hydraulic shear model developed in [144] where the porous medium was represented as a system of parallel capillary tubes. Using this notion, the initiation of particle migration has been modelled as a result of the momentum transfer from the seepage flow flux to the "likely to be mobile" fine particles (silt or clay) present in the internal surfaces of the constrictions—interfacial erosion [141]. Moreover, it has been showed that the shape of the particles and the duration of the experiments governed the energy required for the particle detachment [141]. The higher angularity of the natural soils demands more energy for the detachment [142, 143] whereas spherical particles, such as glass beads, requires lesser energy. Longer durations of the fluid flow, as given in [139], reduce the energy required for particle detachment and it is shown as a reduction in critical hydraulic gradient [47].

The ability of the mechanical stresses to alter the critical hydraulic gradients—the hydromechanical coupling—poses a greater challenge and complexity to the available incomplete knowledge of internal instability. It highlights the dire need for a standardised practice for evaluating the initiation of internal instability. Most of the early studies acknowledged the initiation point of internal instability when even a slight particle suffusion was observed. Conversely, recent studies monitor the temporal variations of the local hydraulic gradients across finite distances along the flow direction to estimate the same: sudden decrease (or increase) defines the initiation point. For instance, [42] considered specimen deformation as a measure of internal instability and showed that the soils that have already experienced internal instability appear to further lose fine particles at an increasing rate with increasing effective stress. Obviously, by definition, their measure of internal instability is the moment when suffusion transforms to suffosion. The increasing loss of fines observed afterwards could be a characteristic of the deformed sample: its volume has changed, and it contains established migration channels from the initial particle suffusion. Thus, integrating such instrumental findings with the existing knowledge on the effects of mechanical and hydraulic stresses in initiating the internal instability becomes extremely challenging, and open to biases, because of the lack of consensus in the experimental methodology.

4.4. Summary of recent developments

Modern numerical and experimental monitoring techniques have enhanced our scientific knowledge on the physics of internal instability phenomenon. Discrete numerical simulation results at the particle level show contrary evidence to the conventional belief of the size-based distinction between the primary fabric and the fines fraction. They prove that the finer particles can also contribute to the force chains, which show the existence of overlapping zones. However, experimental methods are still unable to validate this numerical proof or, on the contrary, accurately discern the primary fabric from the fines fraction (Figure 10). Additionally, extracting undisturbed samples to determine the CSD and the real-time monitoring of particle migration, and post-migration effects is still a major challenge. Taken together, this limitation and the lack of consensus on experimental conditions and practices in measuring the initiation of internal instability hinder the development of a mechanics-based theoretical model for internal instability phenomenon.

DEM simulations of the pore structure are instrumental to relate the particle- scale mechanics of internal instability to its macro-scale manifestations. This level of simulation necessitates substantial computational powers, which is fairly abundant compared to the early days of DEM. Incorporating rotational and frictional forces, natural angularities and shapes of the soil particles into the simulations allows realistic particle movements. It has provided evidence on the transitional nature of suffusion to suffosion, and also an insight into the division of primary and fines fraction, which yet could not be experimentally validated. Additionally, extrapolating the micro-level simulation results to macro-scale engineering applications, such as predicting erosion in earth dams, still remains as a challenge. Improved algorithms and the advances in cloud computing technologies, however, have drastically improved feasibility in increasing the number of particles in the DEM simulations. This has enabled integrating DEM with finite element method (FEM), which is a well-established method to model the continuum scale phenomena.

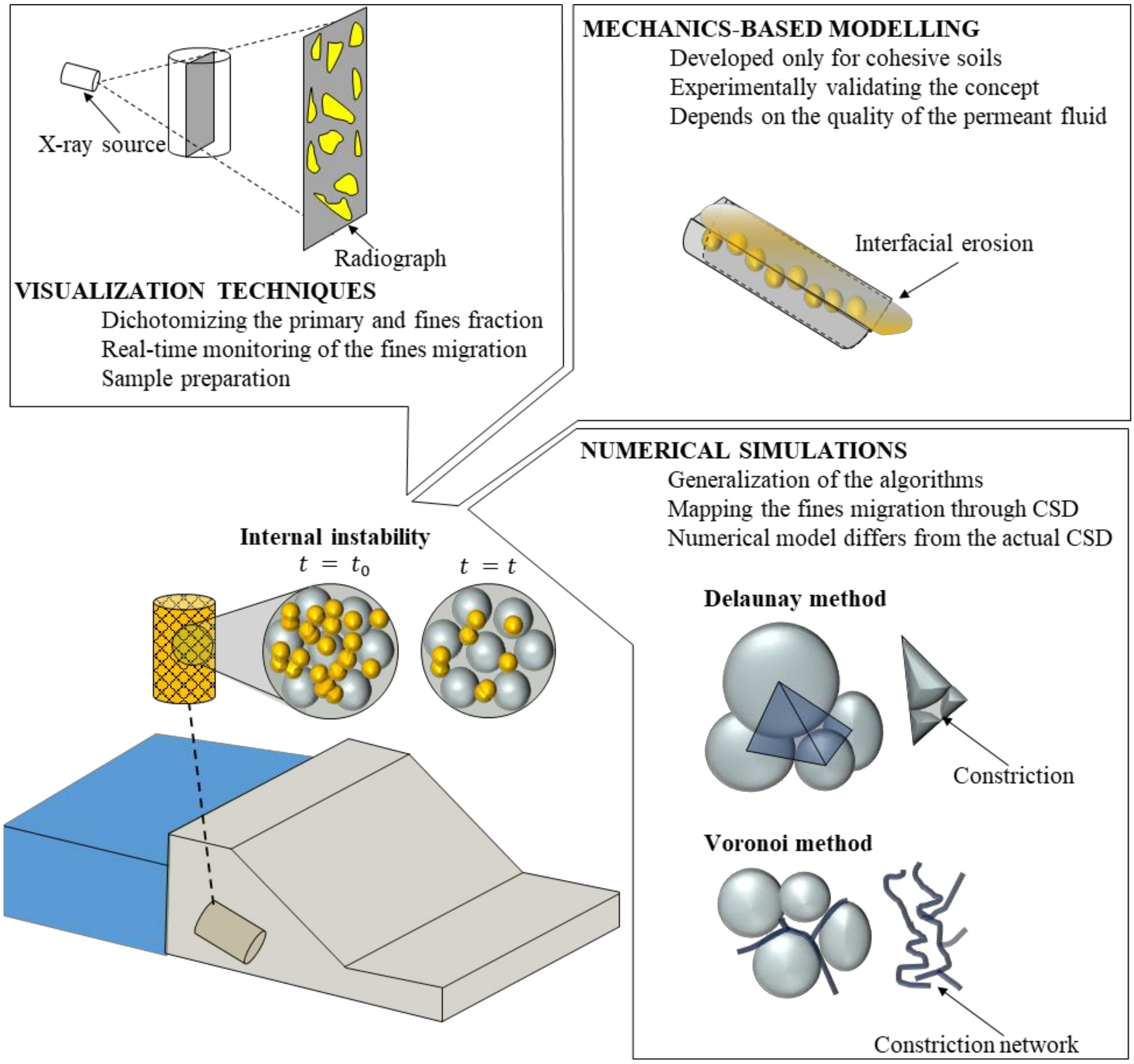

Figure 10. Key challenges faced in the recent developments of internal instability studies.

The use of visualization techniques is comparatively less popular in investigating internal instability, mainly due to the practical difficulties in discerning the primary fabric from the migrating fines fraction. The opaque nature of soils equally poses a greater challenge. X-ray images can only be used to construct the CSD of the soil structure, but they alone cannot be used to map the particle suffusion occurring inside the specimen. Studies that experimentally observe the particle migration used transparent samples/particles or an optically matched permeant fluid other than water. Given the complexity of this phenomenon, it is arguable whether the tracing particles can travel at the same velocity as the migrating particles. Although the applicability of using artificial materials to investigate such a complex physical process is debatable, they can provide instrumental experimental evidence to the internal instability phenomenon in soils at the particle level.

5. Closing thoughts

Internal instability, a characteristic of the soil, progresses as suffusion (or suffosion), becoming a significant cause of failure in geotechnical and transportation infrastructures. The current studies published by the countries with aging geotechnical and transportation infrastructures show disproportionate attention on developing design guidelines and assessment criteria as countermeasures to this nuisance. Complex micro-level interactions and the time-dependent nature of internal instability have been better captured by robust computational techniques, such as DEM. The theoretical understanding of this physical phenomenon, however, has advanced in a relatively modest manner. This trend can be positively altered with the advent of modern experimental visualization and monitoring techniques. To this end, a standardization of the range of experimental conditions is deemed essential.

The classical empirical approaches have focused on selected shapes of PSDs, presumed to be internally unstable. Also, minimal effort has been invested in stimulating field conditions. The extremity of hydraulic and mechanical boundary conditions applied in these experiments highlights that their objectives focused on deriving conservative design measures and assessment criteria. Nevertheless, the geometrical criteria developed using the soil (or soil mixture) PSDs have been satisfactory from a practitioners' perspective. However, the applicability of these empirical criteria in predicting the progression of internal instability on aging geotechnical and transportation infrastructures requires further investigations.

Numerical techniques, such as DEM, can simulate the micro-level particle migration and the resulting inter-particle mechanical stresses. The experimental observations made using X-Ray CT images and tracer particles at a particulate level have confirmed the high accuracy of these simulations. The particle-based numerical methods, however, need greater computational power and optimized algorithms to simulate field-level problems using a larger number of particles aptly. Moreover, experimental techniques that employ X-ray CT images, transparent samples, tracing particles, and modified permeant fluids should be further refined to gain deeper insight into the phenomenon. The prospective studies should explore novel methods to monitor and quantify multi-phase flow patterns, particularly distinguishing mobile fines fraction and the stable primary fabric. Such studies shall enable the researchers to understand more complex physics governing the transitional nature of the internal instability phenomenon.

Data Availability

No data, models, or code were generated or used during the study

Acknowledgements

This work was supported by the Monash Warwick Alliance Catalyst Fund (ENG/Warwick/01-2019/002). The first author acknowledges the financial assistance given by Monash University through the Graduate Research Merit Scholarship.

Compliance with ethics guidelines

All authors declare that they have no conflict of interest or financial conflicts to disclose.

Notation

$(P_N)_i$: probability of occurrence based on number of particles

$(D_c)_3$: constriction size at the densest state

$(D_c)_4$: constriction size at the loosest state

$(P_S)_i$: probability of occurrence based on the contact surface area

μ_{a_w}: attenuation coefficient of pure water

$i_c{}'$: critical hydraulic gradient that triggers internal instability

P_{d_i}: the percent finer by mass for a given particle size d_i

σ'_v: the vertical effective stress

σ'_{vm}: the initial vertical effective stress

μ_a: linear attenuation coefficient of the material

C_u: coefficient of uniformity

D_{CD}: arbitrary constriction size in the densest state

D_{CL}: arbitrary constriction size in the loosest state

$d_{F,X}$: particle size that belongs to fines fraction at X % mass passing

D_F: grain size at F_D % mass passing

d_{max}: maximum size of the fines fraction

D_{min}: minimum size of the coarse fraction

$d_{P,X}$: particle size that belongs to primary fabric at X % mass passing

e_{max}: maximum void ratio of the soil mixture

e_{min}: minimum void ratio of the soil mixture

F_D: mass passing percentage of size D_F

G_r: gap ratio ($G_r = D_{min}/d_{max}$)

G_s: specific gravity of the material or soil

i_c: critical hydraulic gradient of fluidization

i_c'': the i_c' for a soil under anisotropic stress conditions

I_o: the intensity of incident radiation

I_r: ratio between determining particle sizes ($I_r = d_{P,15}/d_{F,85}$)

P_{D_C}: cumulative percentage of constriction size D_C in the CSD

P_C: probability of occurrence of a constriction size D_C

R': hydrodynamic number ($R' = qD_5/\nu n$)

R_d: relative density ($R_d = \frac{(e_{max} - e_M)}{(e_{max} - e_{min})} \times 100$)

S_c: area of the inscribed circle (or the constriction)

γ_s: unit weight of soil

γ_w: unit weight of water at a given temperature

ϕ': the internal effective friction angle of soil

F_n: normal force between particles in contact

F_t: the tangential force between particles in contact

U_n: normal overlapping distance between the two particles

e_s: inter-granular void ratio

k_n: contact normal stiffness

k_{tang}: tangential stiffness

n_f: the ratio between the fines and the coarse fraction

Δu_t: tangential displacement of the two particles in contact

α_n: stiffness ratio

$\Delta\sigma'_v$: deviatoric stress

CSD: Constrictions size distribution

DEM: discrete element method

E: Young's modulus

H: difference between the mass passing percentages at size D_F and $4D_F$ ($H = F_{4D_F} - F_{D_F}$)

h′ ($h' = d_{90}/d_{15}$) and h″($h'' = d_{90}/d_{60}$): conditional factors of uniformity

I: the intensity of transmitted radiation

n: porosity of the soil mixture

PLIF: plane laser induced fluorescence

PSD: particle size distribution

q: unit flux

S: secant slope of the PSD

ν: kinematic viscosity of water at a given temperature

σ′: the confining effective stress on the specimen at the initiation of internal instability

τ: hydraulic shear stresses

ϕ: the internal friction angle of soil

References

[1] Fell R, and Fry JJ. State of the art on the likelihood of internal erosion of dams and levees by means of testing. Erosion in geomechanics applied to dams and levees, pages 1–99, 2013.

[2] Sterpi D. Effects of the erosion and transport of fine particles due to seepage flow. international journal of Geomechanics, 3(1):111–122, 2003.

[3] Johnston I, Murphy W, Holden J. A review of floodwater impacts on the stability of transportation embankments. Earth-Science Reviews. 2021 Feb 6:103553.

[4] Miller GA, Muraleetharan KK, Lim YY. Wetting-induced settlement of compacted-fill embankments. Transportation research record. 2001;1755(1):111-8.

[5] Long JH, Olson SM, Stark TD, Samara EA. Differential movement at embankment-bridge structure interface in Illinois. Transportation Research Record. 1998;1633(1):53-60.

[6] Bian X, Jiang H, Chen Y. Preliminary testing on high-speed railway substructure due to water level changes. Procedia engineering. 2016 Jan 1;143:769-81.

[7] Rönnqvist H, Fannin J, Viklander P. On the use of empirical methods for assessment of filters in embankment dams. Géotechnique Letters, 4(4):272–282, 2014.

[8] Stewart RA, Garner SJ. Performance and Safety of WAC Bennett Dam–a seven year update. InProceedings of the 53rd Canadian Geotechnical Conference, Montréal, Que, pages 15–18, 2000.

[9] Richards KS, Reddy KR. Critical appraisal of piping phenomena in earth dams. Bulletin of Engineering Geology and the Environment, 66(4):381–402, 2007.

[10] Fan X, Dufresne A, Whiteley J, Yunus AP, Subramanian SS, Okeke CA, Pánek T, Hermanns RL, Ming P, Strom A, Havenith HB. Recent technological and methodological advances for the investigation of landslide dams. Earth-Science Reviews. 2021 Apr 22:103646.

[11] Guo Y, Leng W, Nie R, Zhao C, Zhang X. Laboratory evaluation of a new device for water drainage in roadside slope along railway systems. Geotextiles and Geomembranes. 2018 Dec 1;46(6):897-903.

[12] Jung YS, Zollinger DG, Wimsatt AJ. Test method and model development of subbase erosion for concrete pavement design. Transportation research record. 2010 Jan;2154(1):22-31.

[13] Sañudo R, Miranda M, García C, García-Sanchez D. Drainage in railways. Construction and Building materials. 2019 Jun 20;210:391-412.

[14] Indiketiya S, Jegatheesan P, Rajeev P, Kuwano R. The influence of pipe embedment material on sinkhole formation due to erosion around defective sewers. Transportation Geotechnics. 2019 Jun 1;19:110-25.

[15] Beevers L, Douven W, Lazuardi H, Verheij H. Cumulative impacts of road developments in floodplains. Transportation research part D: transport and environment. 2012 Jul 1;17(5):398-404.

[16] Chao Z, Fowmes G, Dassanayake SM. Comparative Study of Hybrid Artificial Intelligence Approaches for Predicting Peak Shear Strength Along Soil-Geocomposite Drainage Layer Interfaces. International Journal of Geosynthetics and Ground Engineering. 2021 Sep;7(3):1-9.

[17] Fell R, Wan CF, Cyganiewicz J, Foster M. Time for development of internal erosion and piping in embankment dams. Journal of geotechnical and geoenvironmental engineering, 129(4):307–314, 2003.

[18] Dassanayake SM, Mousa A. Probabilistic stability evaluation for wildlife-damaged earth dams: a bayesian approach. Georisk: Assessment and Management of Risk for Engineered Systems and Geohazards, 14(1): 41–55, 2020.

[19] Bayoumi A, Meguid MA. Wildlife and safety of earthen structures: a review. Journal of Failure Analysis and Prevention, 11(4): 295–319, 2011.

[20] Cyril G, Yves-Henri F, Rémi B, Chia-Chun H. Contact erosion at the interface between granular coarse soil and various base soils under tangential flow condition. Journal of Geotechnical and Geoenvironmental Engineering, 136:741–750, 2010.

[21] Vakili AH, Shojaei SI, Salimi M, bin Selamat MR, Farhadi MS. Contact erosional behaviour of foundation of pavement embankment constructed with nanosilica-treated dispersive soils. Soils and Foundations. 2020 Feb 1;60(1):167-78.

[22] Fannin RJ, Slangen P, Mehdizadeh A, Disfani MM, Arulrajah A, Evans R. Discussion: On the distinct phenomena of suffusion and suffosion. Géotechnique Letters, 5(3):129– 130, 2015. ISSN 2045-2543. doi: 10.1680/jgele.15.00017. URL http://www.icevirtuallibrary.com/doi/10.1680/jgele.15.00017.

[23] Fannin RJ, Slangen P. On the distinct phenomena of suffusion and suffosion. Géotechnique Letters, 4(4):289–294, sep 2014. ISSN 2045-2543. doi: 10.1680/geolett.14.00051. URL http://www.icevirtuallibrary.com/doi/10.1680/geolett.14.00051.

[24] Moffat R, Fannin RJ, Garner SJ. Spatial and temporal progression of internal erosion in cohesionless soil. Canadian Geotechnical Journal, 48(3):399– 412, 2011. ISSN 0008-3674. doi: 10.1139/T10-071. URL http://www.nrcresearchpress.com/doi/abs/10.1139/T10-071.

[25] Schuler U. Scattering of the composition of soils. An aspect for the stability of granular filters. In Geofilters, pages 21–34, 1996.

[26] Seville JP, Willett CD, Knight PC. Interparticle forces in fluidisation: a review. Powder Technology, 113(3):261–268, 2000.

[27] Zeghal M, El Shamy U. Liquefaction of saturated loose and cemented granular soils. Powder Technology, 184(2):254–265, 2008.

[28] Alsaydalani MO, Clayton CR. Internal fluidization in granular soils. Journal of Geotechnical and Geoenvironmental Engineering, 140 (3):04013024, 2014.

[29] Li M, Fannin RJ. Comparison of two criteria for internal stability of granular soil. Canadian Geotechnical Journal, 45(9):1303– 1309, 2008.

[30] Wan CF, Fell R. Assessing the Potential of Internal Instability and Suffusion in Embankment Dams and Their Foundations. Journal of Geotechnical and Geoenvironmental Engineering, 134(3):401–407, 2008. ISSN 1090-0241. doi: 10.1061/(ASCE)1090-0241(2008)134:3(401).

[31] Richards KS, Reddy KR. Critical appraisal of piping phenomena in earth dams. Bulletin of Engineering Geology and the Environment, 66(4):381–402, 2007. ISSN 14359529. doi: 10.1007/s10064-007- 0095-0.

[32] Kenney TC, Chahal R, Chiu E, Ofoegbu GI, Omange GN, Ume CA. Controlling constriction sizes of granular filters. Canadian Geotechnical Journal, 22(1):32– 43, 1985. ISSN 0008-3674. doi: 10.1139/t85-005. URL http://www.nrcresearchpress.com/doi/10.1139/t85-005.

[33] Indraratna B, Nguyen VT, Rujikiatkamjorn C. Assessing the Potential of Internal Erosion and Suffusion of Granular Soils. Journal of Geotechnical and Geoenvironmental Engineering, 137(5):550–554, 2011. ISSN

[34] Kenney TC, Lau D. Internal stability of granular filters. Canadian Geotechnical Journal, 22(2):215–225, may 1985. ISSN 0008-3674. doi: 10.1139/t85-029. URL http://www.nrcresearchpress.com/doi/abs/10.1139/t85-029.

[35] Moffat RA, Fannin RJ. A large permeameter for study of internal stability in cohesionless soils. Geotechnical Testing Journal, 29(4):273–279, 2006. ISSN 01496115. doi: 10.1520/GTJ100021.

[36] Xiao M, Shwiyhat N. Experimental investigation of the effects of suffusion on physical and geomechanic characteristics of sandy soils. Geotechnical Testing Journal, 35(6):1–11, 2012. ISSN 01496115. doi: 10.1520/GTJ104594.

[37] Bendahmane F, Marot D, Alexis A. Experimental Parametric Study of Suffusion and Backward Erosion. Journal of Geotechnical and Geoenvironmental Engineering, 134(1):57–67, 2008. ISSN 1090-0241. doi: 10.1061/(ASCE)1090-0241(2008)134:1(57).

[38] Frost JD, Park JY. A critical assessment of the moist tamping technique. Geotechnical Testing Journal, 26(1):57–70, 2003.

[39] Moffat R. Experiment on the internal stability of widely graded cohesionless soils. PhD thesis, The University of British Columbia, 2005.

[40] Ke L, Takahashi A. Strength reduction of cohesionless soil due to internal erosion induced by one-dimensional upward seepage flow. Soils and Foundations, 52(4):698–711, 2012.

[41] Chang DS, Zhang LM. A stress-controlled erosion apparatus for studying internal erosion in soils. Geotechnical Testing Journal, 34(6): 103889, jul 2011. ISSN 01496115. doi: 10.1520/GTJ103889.

[42] Chang DS, Zhang LM. Critical Hydraulic Gradients of Internal Erosion under Complex Stress States. Journal of Geotechnical and Geoenvironmental Engineering, 139(9):1454–1467, 2013. ISSN 1090-0241. doi: 10.1061/(ASCE)GT.1943-5606.0000871.

[43] Douglas KJ, Fell R, Peirson WL, Studholme H. Experimental investigation of global backward erosion and suffusion of soils in embankment dams. Canadian Geotechnical Journal, 56(6):789– 807, 2019.

[44] Sail Y, Marot D, Sibille L, Alexis A. Suffusion tests on cohesionless granular matter Suffusion tests on cohesionless granular matter Experimental study. European Journal of Environmental and Civil Engineering, 15(5):799–817, 2011. ISSN 1964-8189. doi: 10.1080/19648189.2011.9693366.

[45] Indraratna B, Israr J, Li M. Inception of geohydraulic failures in granular soils – an experimental and theoretical treatment. Geotechnique, pages 1–16, 2017. ISSN 0016-8505. doi: 10.1680/jgeot.16.P.227.

[46] Rochim A, Marot D, Sibille L, Thao Le V. Effects of Hydraulic Loading History on Suffusion Susceptibility of Cohesionless Soils. Journal of Geotechnical and Geoenvironmental Engineering, 143(7):04017025, 2017.

[47] Dassanayake SM, Mousa A, Sheng LJ, Chian CC. A statistical inference of hydraulic shear and clogging in internally unstable soils. Géotechnique Letters, 10(1):67–72, 2020.

[48] Marot D, Bendahmane F, Nguyen HH. Influence of angularity of coarse fraction grains on internal erosion process. La Houille Blanche, 2012. ISSN 0018-6368. doi: 10.1051/lhb/2012040.

[49] Sterpi D. Effects of the Erosion and Transport of Fine Particles due to Seepage Flow. International Journal of Geomechanics, 3(1):111–122, 2003. ISSN 1532- 3641. doi: 10.1061/(ASCE)1532-3641(2003)3:1(111).

[50] Valdes JR, Santamarina JC. Clogging: bridge formation and vibration-based destabilization. Canadian Geotechnical Journal, 45(2):177–184, 2008. ISSN 0008-3674. doi: 10.1139/T07-088.

[51] Honjo Y, Haque MA, Tsai KA. Self-filtration behaviour of broadly and gap-graded cohesionless soils. In Geofilters, pages 227–236, 1996.

[52] USACE (United States Army Corps of Engineers). Filter experiments and design criteria. Vicksburg, MS: USACE Waterways Experiment Station., 1953.

[53] Åberg B. Washout of Grains from Filtered Sand and Gravel Materials. Journal of Geotechnical Engineering, 119(1):36–53, jan 1993. ISSN 0733-9410. doi: 10.1061/(ASCE)0733-9410(1993)119:1(36).

[54] Burenkova VV. Assessment of suffusion in non-cohesive and graded soils. In Filters in geotechnical and hydraulic engineering., Balkema, Rotterdam, 1993.

[55] Chapuis RP, Contant A, Baass KA. Migration of fines in 0-20 mm crushed base during placement, compaction, and seepage under laboratory conditions. Canadian Geotechnical Journal, 33(1):168–176, 1996. ISSN 0008-3674.

[56] Kaoser S, Barrington S, Elektorowicz M, Ayadat T. The influence of hydraulic gradient and rate of erosion on hydraulic conductivity of sandbentonite mixtures. Soil and Sediment Contamination, 15(5):481–496, oct 2006. ISSN 15320383 15497887. doi: 10.1080/15320380600847815.

[57] Den Adel H, Bakker KJ, Breteler MK. Internal stability of minestone. In Modelling Soil-Water-Structure Interactions, pages 225– 231, Balkema, Rotterdam, 1988.

[58] Lafleur J, Mlynarek J, Rollin AL. Filtration of Broadly Graded Cohession Soils. Journal of Geotechnical Engineering, 115(12):1747–1768, dec 1989. ISSN 0733- 9410. doi: 10.1061/(ASCE)0733-9410(1989)115:12(1747).

[59] Sun BC. Internal stability of clayey to silty sands. PhD thesis, 1990.

[60] Skempton AW, Brogan JM. Experiments on piping in sandy gravels. Géotechnique, 44(3):449–460, sep 1994. ISSN 0016-8505. doi: 10.1680/geot.1994.44.3.449.

[61] Maoxin L. Seepage Induced Instability in Widely Graded Soils. PhD thesis, jan 2008.

[62] Cividini A, Bonomi S, Vignati GC, Gioda G. Seepage-Induced Erosion in Granular Soil and Consequent Settlements. International Journal of Geomechanics, 9(August):187–194, aug 2009. ISSN 15323641.

[63] Lafleur J, Nguyen PH. Internal stability of particles in dam cores made of cohesionless broadly graded moraines. Internal Erosion of Dams and their Foundations., pages 151–158, 2007.

[64] Marot D, Regazzoni PL, Wahl T. Energy-Based Method for Providing Soil Surface Erodibility Rankings. Journal of Geotechnical and Geoenvironmental Engineering, 137(12):1290–1293, dec 2011. ISSN 1090-0241. doi: 10.1061/(ASCE)GT.1943-5606.0000538.

[65] Salehi Sadaghiani MR, Witt KJ. Experimental identification of mobile particles in suffusible non cohesive soils. European Journal of Environmental and Civil Engineering, 15(8):1155–1165, jan 2011. ISSN 1964-8189. doi: 10.1080/19648189.2011.9714846.

[66] Rasheed AK, Dassanayake SM, Mousa A. Suffusion susceptibility in gap-graded granular soils under variable hydraulic loading. In Fifteenth international conference on structural and geotechnical engineering, Cairo, 2018.

[67] Sherard JL. Sinkholes in dams of coarse, broadly graded soils. 13th int. In Congress on Large Dams, New Delhi, page R2, 1979.

[68] Kezdi. Soil physics: selected topics. Elsevier, 1979. ISBN 0444997903. doi: 10.1016/B978-0-444-41728-2.50001-1.

[69] Terrzaghi K. Soil Mechanics: a new Chapter in Engineering Science. Journal of the ICE, 12(7):106–142, jun 1939. ISSN 0368-2455. doi: 10.1680/ijoti.1939.14534.

[70] Sherard JL, Dunnigan LP, Talbot JR. Filters for Silts and Clays. Journal of Geotechnical Engineering, 110(6):701, 1984. ISSN 07339410. doi: 10.1061/(ASCE)0733-9410(1984)110:6(701).

[71] Zhou ZQ, Ranjith PG, Li SC. Criteria for assessment of internal stability of granular soil. Proceedings of the Institution of Civil Engineers-Geotechnical Engineering, 170(1):73–83, 2016.

[72] Liu H, Zou D, Liu J. Particle Shape Effect on Macro-and Micro Behaviours of Monodisperse Ellipsoids. International Journal for Numerical and Analytical Methods in Geomechanics, 32(March 2007):189–213, 2008. ISSN 03639061. doi: 10.1002/nag.

[73] Chapuis RP. Similarity of internal stability criteria for granular soils. Canadian Geotechnical Journal, 29(4):711– 713, 1992. ISSN 0008-3674. doi: 10.1139/t92-078. URL http://www.nrcresearchpress.com/doi/abs/10.1139/t92-078.

[74] Moraci N, Mandaglio MC, Ielo D. Analysis of the internal stability of granular soils using different methods. Canadian Geotechnical Journal, 51(9):1063–1072, 2014.

[75] Li M, Fannin RJ. Comparison of two criteria for internal stability of granular soil. Canadian Geotechnical Journal, 45 (9):1303–1309, 2008. ISSN 0008-3674. doi: 10.1139/T08-046. URL http://www.nrcresearchpress.com/doi/abs/10.1139/T08-046.

[76] Mousa A, Youssef TA. Genesis of transitional behaviour in geomaterials: a review and gap analysis. Geomechanics and Geoengineering, pages 1–27, 2019.

[77] Chang DS, Zhang LM. Extended internal stability criteria for soils under seepage. Soils and Foundations, 53(4):569–583, 2013. ISSN 00380806. doi: 10.1016/j.sandf.2013.06.008.

[78] Yang KH, Wang JY. Experiment and statistical assessment on piping failures in soils with different gradations. Marine Georesources & Geotechnology, 35(4):512–527, 2017.

[79] Bonelli S, Marot D. Micromechanical modeling of internal erosion. European Journal of Environmental and Civil Engineering, 158(August 2013):1207–1224, jan 2011. ISSN 1964-8189. doi: 10.1080/19648189.2011.9714849.

[80] Silveira A, de Lorena Peixoto T, Nogueira J. On void size distribution of granular materials. In the 5th Pan American Conference on Soil Mechanics and Foundation Engineering, pages 161–177, Buenos Aires, 1975.

[81] To HD, Scheuermann A, Galindo-Torres SA. Probability of Transportation of Loose Particles in Suffusion Assessment by Self-Filtration Criteria. Journal of Geotechnical and Geoenvironmental Engineering, 2016. ISSN 1090-0241. doi: 10.1061/(ASCE)GT.1943-5606.0001403.

[82] Vincens E, Witt KJ, Homberg U. Approaches to determine the constriction size distribution for understanding filtration phenomena in granular materials. Acta Geotechnica. 2015 Jun;10(3):291-303.

[83] Reboul N, Vincens E, Cambou B. A statistical analysis of void size distribution in a simulated narrowly graded packing of spheres. Granular Matter, 10(6):457–468, 2008. ISSN 14345021. doi: 10.1007/s10035-008-0111-5.

[84] Scheuermann A, Bieberstein A. Determination of the Soil Water Retention Curve and the Unsaturated Hydraulic Conductivity from the Particle Size Distribution. Experimental Unsaturated Soil Mechanics, Springer Proceedings in Physics Volume 112, 112:421–433, 2007. doi: 10.1007/3-540- 69873-6. URL http://link.springer.com/10.1007/3-540-69873-6 42 http://link.springer.com/chapter/10.1007/3-540-69873-6 42.

[85] Shire T, O'Sullivan C. A network model to assess basefilter combinations. Computers and Geotechnics, 84:117–128, 2017. ISSN 18737633. doi: 10.1016/j.compgeo.2016.11.014. URL http://dx.doi.org/10.1016/j.compgeo.2016.11.014.

[86] Humes C. A new approach to compute the void size distribution curves of protective filters. In Geofilters, pages 57–66, 1996.

[87] Raut AK. Mathematical modelling of granular filters and constriction-based filter design criteria. PhD thesis, University of Wollongong, 2006.

[88] Locke M, Indraratna B, Adikari G. Time-Dependent Particle Transport through Granular Filters. Journal of Geotechnical and Geoenvironmental Engineering, 127(6):521–529, 2001. ISSN 1090-0241. doi: 10.1061/(ASCE)1090-0241(2001)127:6(521).

[89] Silveira A. An analysis of the problem of washing through in protective filters. In The 6th International Conference on Soil Mechanics and Foundation Engineering, pages 551–555, Montr´eal, 1965.

[90] Soria M, Aramaki R, Viviani E. Experimental determination of void size curves. Filters in geotechnical and hydraulic engineering, pages 43–48, 1993.

[91] Indraratna B, Israr J, Rujikiatkamjorn C. Geometrical Method for Evaluating the Internal Instability of Granular Filters Based on Constriction Size Distribution. Journal of Geotechnical and Geoenvironmental Engineering, 141(10):04015045, 2015. ISSN 1090-0241. doi: 10.1061/(ASCE)GT.1943-5606.0001343.

[92] Bonelli S, Nicot F. Erosion in Geomechanics Applied to Dams and Levees. 2013. ISBN 9781848214095. doi: 10.1002/9781118577165.

[93] Shire T, O'Sullivan C. Micromechanical assessment of an internal stability criterion. Acta Geotechnica, 8(1):81–90, 2013. ISSN 18611125. doi: 10.1007/s11440-012-0176-5.

[94] Blunt MJ, Bijeljic B, Dong H, Gharbi O, Iglauer S, Mostaghimi P, Paluszny A, Pentland C. Pore-scale imaging and modelling. Advances in Water Resources, 51:197–216, jan 2013. ISSN 03091708. doi: 10.1016/j.advwatres.2012.03.003. URL http://linkinghub.elsevier.com/retrieve/pii/S0309170812000528.

[95] Macedo A, Vaz CM, Naime JM, Cruvinel PE, Crestana S. X-ray microtomography to characterize the physical properties of soil and particulate systems. Powder technology, 101(2):178–182, 1999.

[96] Tsuji Y, Kawaguchi T, Tanaka T. Discrete particle simulation of two-dimensional fluidized bed. Powder Technology, 77(1):79–87, oct 1993. ISSN 00325910. doi: 10.1016/0032-5910(93)85010-7.

[97] Coetzee CJ. Calibration of the discrete element method. Powder Technology, 310:104–142, 2017.

[98] Langroudi MF, Soroush A, Shourijeh PT. A comparison of micromechanical assessments with internal stability/instability criteria for soils. Powder Technology, 276:66–79, 2015.

[99] Reboul N, Vincens E, Cambou B. A computational procedure to assess the distribution of constriction sizes for an assembly of spheres. Computers and Geotechnics, 37(1-2):195–206, jan 2010. ISSN 0266352X.

[100] Al-Raoush R, Thompson K, Willson CS. Comparison of network generation techniques for unconsolidated porous media. Soil Science Society of America Journal, 67(6):1687, nov 2003. ISSN 1435-0661. doi: 10.2136/sssaj2003.1687.

[101] Wautier A, Bonelli S, Nicot F. Dem investigations of internal erosion: Grain transport in the light of micromechanics. International Journal for Numerical and Analytical Methods in Geomechanics, 43(1):339–352, 2019.

[102] Kozicki J, Donze FV. Yade-open dem: An open-source software using a discrete element method to simulate granular material. Engineering Computations, 2009.

[103] Luchnikov VA, Gavrilova ML, Medvedev NN, Voloshin VP. The Voronoi-Delaunay approach for the free volume analysis of a packing of balls in a cylindrical container. Future Generation Computer Systems, 18(5):673–679, 2002. ISSN 0167739X.

[104] To HD, Torres SA, Scheuermann A. Primary fabric fraction analysis of granular soils. Acta Geotechnica, 10 (3):375–387, 2015.

[105] Shire T, O'Sullivan C. Constriction size distributions of granular filters: a numerical study. Géotechnique, 66(10):826– 839, 2016. ISSN 0016-8505.

[106] Peters JF, Berney IV ES. Percolation threshold of sand-clay binary mixtures. Journal of geotechnical and geoenvironmental engineering. 2010 Feb;136(2):310-8.

[107] Yamamuro JA, Lade PV. Steady-state concepts and static liquefaction of silty sands. Journal of geotechnical and geoenvironmental engineering. 1998 Sep;124(9):868-77.

[108] Simpson DC, Evans TM. Behavioral thresholds in mixtures of sand and kaolinite clay. Journal of Geotechnical and Geoenvironmental Engineering. 2016 Feb 1;142(2):04015073.

[109] Consiglio R, Baker DR, Paul G, Stanley HE. Continuum percolation thresholds for mixtures of spheres of different sizes. Physica A: Statistical Mechanics and its Applications. 2003 Mar 1;319:49-55.

[110] Sahimi M. Long-range correlated percolation and flow and transport in heterogeneous porous media. Journal de Physique I. 1994 Sep 1;4(9):1263-8.

[111] Mousa A. The “gray zone”: fabric and consistency of natural transitional soils. Arabian Journal of Geosciences. 2016 Jan;9(1):1-6.

[112] Pandian NS, Nagaraj TS, Raju PN. Permeability and compressibility behavior of bentonite-sand/soil mixes. Geotechnical Testing Journal. 1995 Mar 1;18(1):86-93.

[113] Lee JS, Dodds J, Santamarina JC. Behavior of rigid-soft particle mixtures. Journal of materials in civil engineering. 2007 Feb;19(2):179-84.

[114] Zhang J, Chen X, Zhang J, Wang X. Microscopic investigation of the packing features of soft-rigid particle mixtures using the discrete element method. Advanced Powder Technology. 2020 Jul 1;31(7):2951-63.

[115] Langroudi MF, Soroush A, Shourijeh PT, Shafipour R. Stress transmission in internally unstable gap-graded soils using discrete element modeling. Powder technology, 247: 161–171, 2013.

[116] Cundall PA, Strack OD. A discrete numerical model for granular assemblies. Géotechnique, 29(1):47–65, 1979. ISSN 0016-8505. doi: 10.1680/geot.1979.29.1.47.

[117] Rosenbrand E. Investigation into quantitative visualisation of suffusion. 2011.

[118] Parker DJ, Forster RN, Fowles P, Takhar PS. Positron emission particle tracking using the new Birmingham positron camera. Nuclear Instruments and Methods in Physics Research Section A: Accelerators, Spectrometers, Detectors and Associated Equipment, 477(1-3):540–545, 2002.

[119] Hernández LG, Pérez JG, Gaytán-Martínez M. Tracers used in granular systems. Powder Technology, 340:274–289, 2018.

[120] Ilankoon IMSK, Cole KE, Neethling SJ. Measuring hydrodynamic dispersion coefficients in unsaturated packed beds: Comparison of PEPT with conventional tracer tests. Chemical Engineering Science, 89:152–157, 2013.

[121] Ilankoon IMSK. Hydrodynamics of unsaturated particle beds pertaining to heap leaching. 2012.

[122] Rosenbrand E, Dijkstra J. Application of image subtraction data to quantify suffusion. Géotechnique Letters, 2:37–41, 2012.

[123] Hunter RP, Bowman ET. Visualisation of seepage-induced suffusion and suffosion within internally erodible granular media. Géotechnique, pages 1–13, 2018.

[124] Cnudde V, Boone MN. High-resolution X-ray computed tomography in geosciences: A review of the current technology and applications. Earth-Science Reviews, 123:1–17, 2013.

[125] Dong H, Blunt MJ. Pore-network extraction from micro-computerized-tomography images. Physical Review E - Statistical, Nonlinear, and Soft Matter Physics, 80(3):036307, sep 2009. ISSN 15393755. doi: 10.1103/PhysRevE.80.036307.

[126] Taud H, Martinez-Angeles R, Parrot JF, Hernandez-Escobedo L. Porosity estimation method by x-ray computed tomography. Journal of petroleum science and engineering, 47(3-4):209–217, 2005.

[127] McCullough EC. Photon attenuation in computed tomography. Medical Physics, 2(6):307–320, 1975.

[128] Dassanayake SM. An Integrated Experimental and Statistical Approach for Predicting the Progression of Internal Instability in Gap-Graded Granular Soils. PhD thesis, Monash University.

[129] Fonseca J, O'sullivan C, Coop MR, Lee PD. Non-invasive characterization of particle morphology of natural sands. Soils and Foundations, 2012. ISSN 00380806. doi: 10.1016/j.sandf.2012.07.011.

[130] Andò E, Hall SA, Viggiani G, Desrues J, Bésuelle P. Grain-scale experimental investigation of localised deformation in sand: a discrete particle tracking approach. Acta Geotechnica, 7(1):1–13, 2012.

[131] van der Linden JH, Narsilio GA, Tordesillas A. Machine learning framework for analysis of transport through complex networks in porous, granular media: A focus on permeability. Physical Review E, 94(2):022904, 2016. ISSN 2470-0045. doi: 10.1103/PhysRevE.94.022904.

[132] Harshani HM, Galindo-Torres SA, Scheuermann A, Muhlhaus HB. Experimental study of porous media flow using hydro-gel beads and led based PIV. Measurement Science and Technology, 28(1):015902, 2016.

[133] Moffat R, Fannin RJ. A hydromechanical relation governing internal stability of cohesionless soil. Canadian Geotechnical Journal, 48(3):413–424, 2011. ISSN 0008-3674. doi: 10.1139/T10-070.

[134] Chang DS, Zhang LM. A Stress-controlled Erosion Apparatus for Studying Internal Erosion in Soils. Geotechnical Testing Journal, 34(6): 1–11, 2011.

[135] Moffat R, Herrera P. Hydromechanical model for internal erosion and its relationship with the stress transmitted by the finer soil fraction. Acta Geotechnica, 10(5):643–650, 2015.

[136] Liang Y, Yeh TC, Wang J, Liu M, Zha Y, Hao Y. Onset of suffusion in upward seepage under isotropic and anisotropic stress conditions. European Journal of Environmental and Civil Engineering, 8189(August):1–15, 2017. ISSN 1964-8189. doi: 10.1080/19648189.2017.1359110.

[137] Thevanayagam S, Mohan S. Intergranular state variables and stress– strain behaviour of silty sands. Geotechnique, 50(1):1–23, 2000.

[138] Yang J, Wei LM, Dai BB. State variables for silty sands: Global void ratio or skeleton void ratio? Soils and Foundations, 55(1):99–111, 2015.

[139] Luo YL, Qiao L, Liu XX, Zhan ML, Sheng JC. Hydro-mechanical experiments on suffusion under long-term large hydraulic heads. Natural Hazards, 65(3):1361–1377, 2013. ISSN 0921030X. doi: 10.1007/s11069-012-0415-y.

[140] Saghaee G, Mousa AA, Meguid MA. Meguid. Plausible failure mechanisms of wildlife-damaged earth levees: insights from centrifuge modeling and numerical analysis. Canadian Geotechnical Journal, 54(10):1496–1508, oct 2017. ISSN 0008-3674. doi: 10.1139/cgj-2016-0484.

[141] Bonelli S, Marot D. On the modelling of internal soil erosion. In The 12th International Conference of International Association for Computer Methods and Advances in Geomechanics (IACMAG), pages 7, 2008.

[142] Marot D, Rochim A, Nguyen HH, Bendahmane F, Sibille L. Assessing the susceptibility of gap-graded soils to internal erosion: proposition of a new experimental methodology. Natural Hazards, 83(1):365–388, 2016. ISSN 15730840. doi: 10.1007/s11069-016-2319-8.

[143] Marot D, Le VD, Garnier J, Thorel L, Audrain P. Study of scale effect in an internal erosion mechanism: centrifuge model and energy analysis. European Journal of Environmental and Civil Engineering, 16(1):1–19, 2012. ISSN 1964-8189. doi: 10.1080/19648189.2012.667203.

[144] Reddi LN, Ming X, Hajra MG, Lee IM. Permeability Reduction of Soil Filters due to Physical Clogging. Journal of Geotechnical and Geoenvironmental Engineering, 126(3):236–246, 2000. ISSN 1090-0241. doi: 10.1061/(ASCE)1090-0241(2000)126:3(236).